reading the manuscript and for very helpful discussions. We also thank Profs. Rafael Ibáñez and José V. Folgado of the University of Valencia for running the curve-fitting programs and for technical assistance in the preliminary ESR experiments. The research was aided by NSF Grant CHE-8406088, by the U. S.-Spain Joint Committee for Scientific Cooperation through Grant CCB-8504039, and by an instrument grant from the W. M. Keck Foundation.

Observation of Anion Spinning in the Dynamic ^{31}P NMR Spectra of Fluorine-Bridged SbF_6^-, BF_4^-, and PF_6^- Adducts of $R_3P(CO)_3(NO)W^+$. Implications for Barriers to Ionization and the Formation of Ion Pairs and Free Ions in Methylene Chloride and Hexane Solution

Robert V. Honeychuck and William H. Hersh*

Contribution from the Department of Chemistry and Biochemistry, University of California, Los Angeles, California 90024-1569. *Received August 12, 1988*

Abstract: An NMR method to measure ionization and ion-pair separation barriers is described. Variable-temperature ^{31}P NMR spectra on *mer*-(*cis*-R_3P)$(CO)_3(NO)W(\mu$-F)EF_n (EF_n = SbF_5, R = Me (**1a**), *n*-octyl (**1b**); R = Me, EF_n = BF_3 (**2**), PF_5 (**3**)) reveal two EF_{n+1}^- exchange processes in methylene chloride and hexane; rate constants are determined from line-shape analyses and the corresponding activation parameters are derived. The low-temperature intramolecular exchange process gives a doublet for the R_3P phosphorus atom due to coupling to the μ-F ligand in the slow-exchange limit, and a septet for **1a**, **1b**, and **3**, and a quintet for **2**, in the fast-exchange limit due to anion "spinning"; the same process gives a doublet of sextets for the PF_6^- phosphorus atom of **3** in the slow-exchange limit and a septet in the fast-exchange limit. The high-temperature intermolecular exchange process results in collapse of each R_3P multiplet to a singlet. For the low-temperature process $\Delta G^{\ddagger}$ follows the expected order SbF_6^- (10.4 kcal/mol for **1a**) > BF_4^- (9.8 kcal/mol) > PF_6^- (9.1 kcal/mol). Two isokinetic reaction series are found for intramolecular exchange, one for Me_3P adducts **1a**, **2**, and **3** in methylene chloride, and one for the SbF_6^- adducts **1a** and **1b** in both methylene chloride and hexane. In the former case decreased anion coordinating ability causes the transition state to move toward lower enthalpy and entropy, while in the latter case the same result is effected by increased steric bulk and lower solvent polarity. For each reaction the intramolecular $\Delta H^{\ddagger}$ is higher than that for the corresponding intermolecular process; essentially similar activation parameters are observed for each high-temperature reaction, with $\Delta H^{\ddagger} \approx 5.6$ kcal/mol and $\Delta S^{\ddagger} \approx -35$ eu. These data are consistent with W-F bond cleavage in the low-temperature process to give ion pairs, followed by ion-pair separation to give free ions in the high-temperature process. This ionization scheme is consistent with theoretical calculations of dissociation constants for formation of free ions from ion pairs in methylene chloride, but not in hexane. A different mechanism is proposed for this latter case, namely, bimolecular anion exchange in reversed micelles of **1b**. A complete free energy and enthalpy diagram is constructed for the methylene chloride ionizations.

Investigation of ionization and ion-pairing phenomena continues to be an area of active research, despite work going back over half a century.[1-12] As illustrated in Scheme I, current interest centers

Scheme I

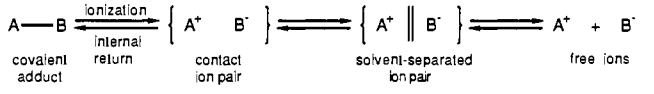

on rates of ionization of the covalent adduct to give contact and/or solvent-separated ion pairs, and rates of separation of the ion pairs via diffusion of the individual ions out of the solvent cage to give the free ions. The existence of such measurable rates implies that the ion pair exists as a true intermediate having a barrier to

(1) Bjerrum, N. *Kgl. Danske Vidensk. Selskab.* **1926**, 7, No. 9. Cf.: Harned, H. S.; Owen, B. B. *The Physical Chemistry of Electrolyte Solutions*, 3rd ed.; Reinhold: New York, 1958; pp 70-74.

(2) (a) Fuoss, R. M.; Kraus, C. A. *J. Am. Chem. Soc.* **1933**, *55*, 1019-1028. (b) Fuoss, R. M. *Ibid.* **1958**, *80*, 5059-5061. (c) Sadek, H.; Hirsch, E.; Fuoss, R. M. In *Electrolytes*; Pesce, B., Ed.; Pergamon Press: Oxford, 1962; pp 132-145. (d) Petrucci, S. In *Ionic Interactions*; Petrucci, S., Ed.; Academic Press: New York, 1971; Vol. I, Chapter 3.

(3) (a) Winstein, S.; Clippinger, E.; Fainberg, A. H.; Robinson, G. C. *J. Am. Chem. Soc.* **1954**, *76*, 2597-2598. (b) Winstein, S.; Clippinger, E.; Fainberg, A. H.; Heck, R.; Robinson, G. C. *Ibid.* **1956**, *78*, 328-335. (c) Fainberg, A. H.; Winstein, S. *Ibid.* **1956**, *78*, 2767-2770. (d) Winstein, S.; Clippinger, E. *Ibid.* **1956**, *78*, 2784-2788. (e) Winstein, S.; Klinedinst, P. E., Jr.; Robinson, G. C. *Ibid.* **1961**, *83*, 885-895.

(4) Lichtin, N. N. *Progr. Phys. Org. Chem.* **1963**, *1*, 75-108.

(5) (a) Carvajal, C.; Tölle, K. J.; Smid, J.; Szwarc, M. *J. Am. Chem. Soc.* **1965**, *87*, 5548-5553. (b) Hogen-Esch, T. E.; Smid, J. *Ibid.* **1966**, *88*, 307-318. (c) Hogen-Esch, T. E.; Smid, J. *Ibid.* **1966**, *88*, 318-324. (d) Slates, R. V.; Szwarc, M. *Ibid.* **1967**, *89*, 6043-6050. (e) Grutzner, J. B.; Lawlor, J. M.; Jackman, L. M. *Ibid.* **1972**, *94*, 2306-2315.

(6) (a) Diaz, A. F.; Lazdins, I.; Winstein, S. *J. Am. Chem. Soc.* **1968**, *90*, 1904-1905. (b) Paradisi, C.; Bunnett, J. F. *Ibid.* **1985**, *107*, 8223-8233.

(7) (a) Ford, W. T.; Cram, D. J. *J. Am. Chem. Soc.* **1968**, *90*, 2612-2622. (b) Almy, J.; Cram. D. J. *Ibid.* **1969**, *91*, 4459-4468. (c) Almy, J.; Hoffman, D. H.; Chu, K. C.; Cram, D. J. *Ibid.* **1973**, *95*, 1185-1190.

(8) (a) Feigel, M.; Kessler, H. *Angew. Chem., Int. Ed. Engl.* **1977**, *16*, 256-257. (b) Feigel, M.; Kessler, H. *Chem. Ber.* **1978**, *111*, 1659-1669. (c) Feigel, M.; Kessler, H. *Ibid.* **1979**, *112*, 3715-3722. (d) Kessler, H.; Feigel, M. *Acc. Chem. Res.* **1982**, *15*, 2-8.

(9) (a) Jencks, W. P. *Acc. Chem. Res.* **1980**, *13*, 161-169. (b) Knier, B. L.; Jencks, W. P. *J. Am. Chem. Soc.* **1980**, *102*, 6789-6798.

(10) (a) Simon, J. D.; Peters, K. S. *J. Am. Chem. Soc.* **1981**, *103*, 6403-6406. (b) Simon, J. D.; Peters, K. S. *Ibid.* **1983**, *105*, 4875-4882. (c) Goodman, J. L.; Peters, K. S. *Ibid.* **1985**, *107*, 6459-6463. (d) Masnovi, J. M.; Kochi, J. K. *Ibid.* **1985**, *107*, 7880-7893. (e) Goodman, J. L.; Peters, K. S. *Ibid.* **1986**, *108*, 1700-1701.

(11) (a) Svorstøl, I.; Høiland, H.; Songstad, J. *Acta Chem. Scand.* **1984**, *B38*, 885-893. (b) Svorstøl, I.; Songstad, J. *Ibid.* **1985**, *B39*, 639-655. (c) Gestblom, B.; Songstad, J. *Ibid.* **1987**, *B41*, 396-409.

(12) See also: (a) Szwarc, M. In *Ions and Ion Pairs in Organic Reactions*; Szwarc, M., Ed.; Wiley: New York, 1972; Vol. 1, Chapter 1. (b) Raber, D. J.; Harris, J. M.; Schleyer, P. v. R. *Ibid.* 1974; Vol. 2, Chapter 3. (c) Grunwald, E.; Highsmith, S.; I, T.-P. *Ibid.* 1974; Vol. 2, Chapter 5. (d) Abraham, M. H. *Progr. Phys. Org. Chem.* **1974**, *11*, 1-87. (e) Bentley, T. W.; Schleyer, P. v. R. *Adv. Phys. Org. Chem.* **1977**, *14*, 1-67. (f) Hogen-Esch, T. E. *Ibid.* **1977**, *15*, 153-266. (g) Brändström, A. *Ibid.* **1977**, *15*, 267-330. (h) Arnett, E. M; Hofelich, T. C.; Schriver, G. W. *React. Intermed.* **1985**, *3*, 189-226.

0002-7863/89/1511-6056$01.50/0

Scheme II

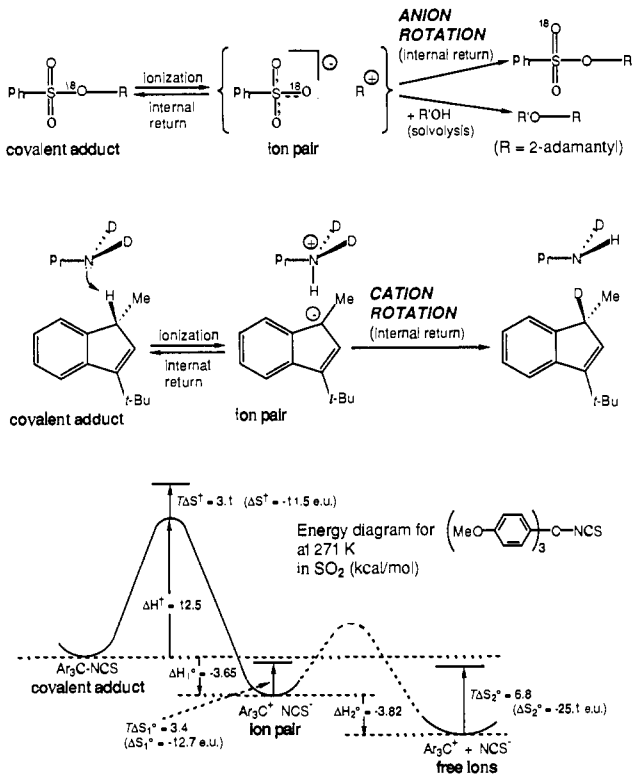

recombination and is not simply a transition state. In Scheme II we illustrate three specific examples of reactions designed to examine some of these factors. The first is a device used by Winstein and most recently Bunnett[6] to study the intermediacy of ion pairs in organic solvolyses; it involves oxygen isotope scrambling during the solvolysis of labeled sulfonate esters, in which formation of ion pairs followed by rotation of the sulfonate ion prior to internal return allows for a random reattachment of oxygen atoms in the covalent adduct. While the possibility exists that scrambling could occur without the intermediacy of an ion pair (that is, by the carbon atom effectively "hopping" from one oxygen atom to another), such a nonionic and presumably concerted process would be expected to be insensitive to solvent polarity, in contrast to the observed results. In the second reaction, due to Cram,[7] proton exchange is mediated by primary amines, and the similarity derives from the fact that ion pair formation is followed by rotation of the ammonium ion. Kessler[8] has reported a series of elegant studies in which the stability of the covalent adduct is similar to that of the ion pair and free ions, thereby allowing the use of dynamic NMR to yield both kinetic and thermodynamic parameters as illustrated for the ionization of tris(4-methoxyphenyl)methyl isothiocyanate.

We recently reported the syntheses, X-ray structures, and ^{19}F and ^{31}P NMR spectra of several tungsten nitrosyl adducts of the "noncoordinating" ions SbF_6^-, BF_4^-, and PF_6^-, namely, *mer*-(*cis*-R_3P)$(CO)_3(NO)W(\mu\text{-}F)EF_n$ (R_3P = Me_3P, Me_2PhP, (cyclohexyl)$_3P$, EF_n = SbF_5; R_3P = Me_3P, EF_n = BF_3, PF_5).[13] The ^{31}P NMR spectra in particular revealed *two* temperature-dependent processes, one corresponding to *intra*molecular anion spinning in which all the fluorine atoms exchange into the bridging site, and the other to *inter*molecular anion exchange. As shown in Scheme III, the former process could be due to ionization to contact ion pairs (in which the identity of the unique bridging fluorine atom is lost) followed by internal return, while the latter process could then simply be due to diffusion of the ions away from each other to give the free ions. Thus, these compounds may be *inorganic* analogues of the rotating sulfonate and ammonium ions in Scheme II; intermolecular anion exchange in the tungsten

(13) (a) Hersh, W. H. *J. Am. Chem. Soc.* **1985**, *107*, 4599–4601. (b) Honeychuck, R. V.; Hersh, W. H. *Inorg. Chem.*, in press.

Scheme III

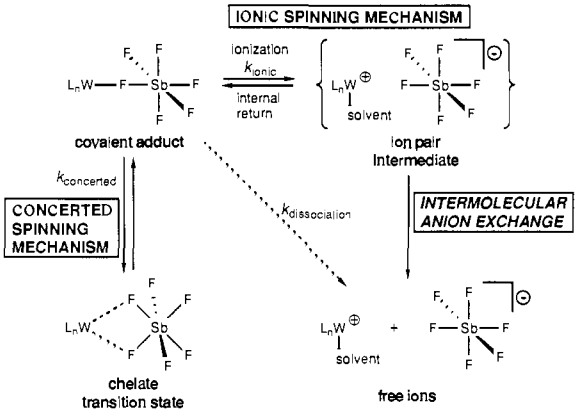

case would correspond to "solvolysis". One difference between the organic and inorganic examples is that solvent coordination to tungsten can occur in the ion pair (as shown in Scheme III), and certainly is expected to occur in the free ions. Another difference is that in the inorganic case the nonionic concerted process shown in Scheme III does not seem so objectionable, since tungsten "hopping" from fluorine to fluorine could occur via a chelate transition state that has ground-state structural analogues such as those shown below,[14] of which the silver PF_6^- adduct and

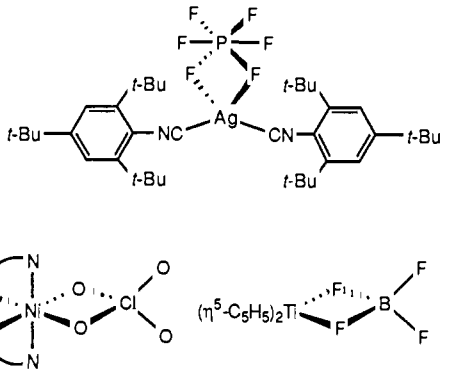

nickel ClO_4^- adducts have been characterized by X-ray crystallography. Nevertheless, the direct NMR observation of the two exchange processes in the tungsten nitrosyl adducts, of which the intermolecular process seemingly *must* involve ionization, provides a unique opportunity to measure rates and hence activation barriers in inorganic systems that have direct analogy to some venerable organic systems; in contrast to Kessler's system in Scheme II, thermodynamic considerations of ionic equilibria do not play a role here and so a wider range of conditions may be available. In this paper we describe temperature-dependent rate data for the two exchange reactions of the "noncoordinating" anion adducts **1a**,[13a] **1b**, **2**, and **3** in several relatively nonpolar solvents, and show

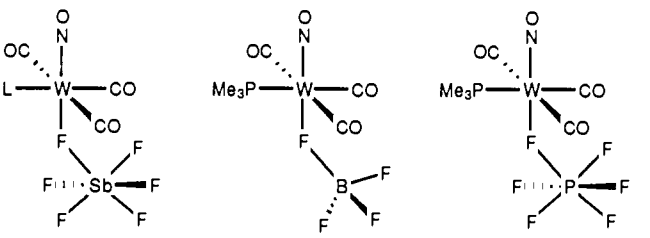

1a L=Me_3P
1b L=*n*-octyl$_3P$ **2** **3**

how the activation barriers are due to ionization and ion-pair

(14) (a) Yamamoto, Y.; Aoki, K.; Yamazaki, H. *Inorg. Chim. Acta* **1982**, *68*, 75–78. (b) House, D. A.; Steel, P. J.; Watson, A. A. *J. Chem. Soc., Chem. Commun.* **1987**, 1575–1576. (c) Nöth, H.; Hartwimmer, R. *Chem. Ber.* **1960**, *93*, 2246–2251.

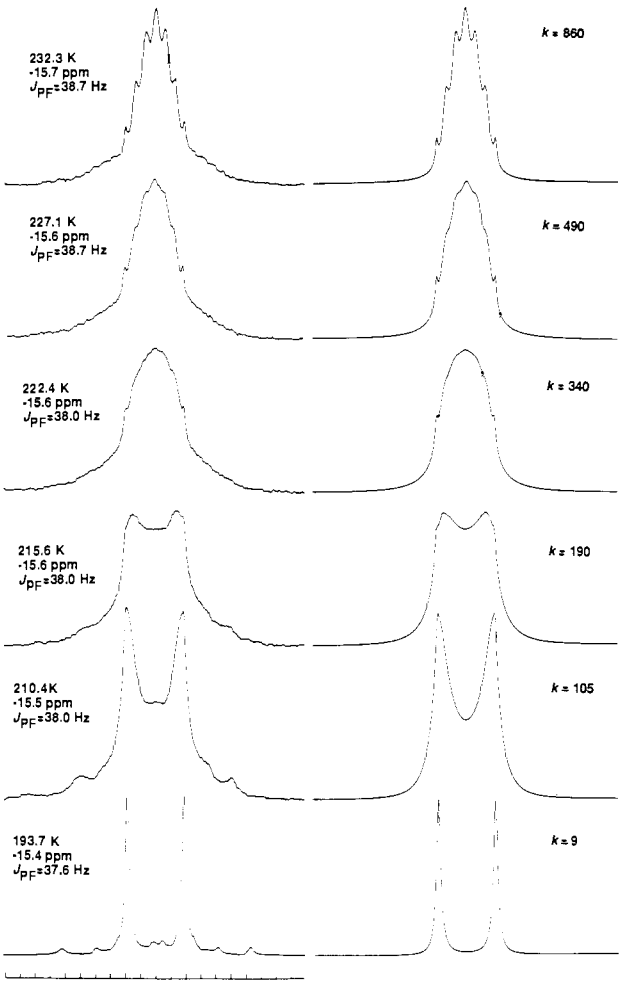

Figure 1. Variable-temperature ^{31}P NMR spectra of **1a** on the left (scale markings are at 10-Hz intervals) and best-fit theoretical spectra (rate constants in s^{-1} for the ionic spinning mechanism) on the right, for intramolecular anion exchange. The small peaks within ±70 Hz of the center of the multiplets, most clearly visible at the two lowest temperatures, were shown to be spinning side bands by varying the spin rate.

separation. Key features include the structure of the ion pair, observation of two isokinetic series, and the surprising result that even in hexane intermolecular anion exchange is observed. A comparison of the rate data to theoretical barriers for formation of free ions as a function of dielectric constant suggests, however, that in hexane intermolecular exchange should not occur via the free ions, so alternatives will be discussed.

Results

Qualitative Observations in CD_2Cl_2. The ^{31}P NMR spectra of **1a** in CD_2Cl_2, taken at temperatures ranging from ~190 to 250 K, are shown in Figure 1, and from ~265 to 345 K in Figure 2; the best fit theoretical line shapes (see below) are shown alongside each spectrum. At the lowest temperature, a clean doublet (apart from the small spinning side bands) is observed, due to coupling between the Me_3P phosphorus atom and the bridging fluorine atom of the SbF_6^- ligand; the longer range coupling constant between the five terminal fluorine atoms and the phosphorus atom is evidently zero. Upon warming, broadening of the doublet is observed as signal intensity grows in between the two original lines of the doublet, with eventual sharpening to a clean *septet* at ~250 K. While it is convenient to state that such a result requires all six fluorine atoms to be equivalent with respect to the phosphorus atom, it is more accurate to simply state that in the fast-exchange limit at 250 K all six fluorine atoms are exchanging into the bridging site. Another obvious point is that this "spinning" process, regardless of the mechanism of exchange, is *intramolecular*. Upon continued warming, the septet collapses to a singlet, as seen in Figure 2. Loss of coupling between the phosphorus and fluorine

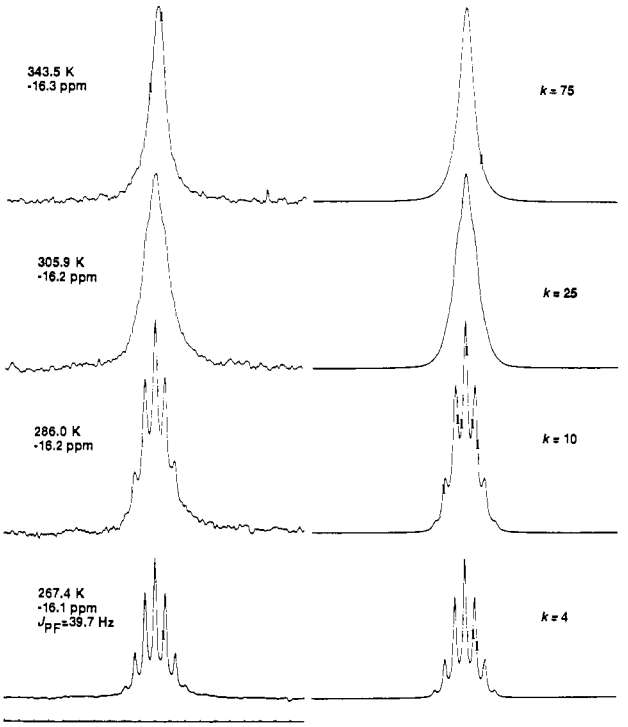

Figure 2. Variable-temperature ^{31}P NMR spectra of **1a** on the left (scale markings are at 10-Hz intervals) and best-fit theoretical spectra (rate constants in s^{-1}) on the right, for intermolecular anion exchange.

atoms can only arise due to cleavage of the tungsten–fluorine bond (there is absolutely no evidence of PMe_3 dissociation) and concomitant *intermolecular* exchange of SbF_6^- ligands. All changes are reversible, and the constancy of the chemical shift is good evidence that the observed species is in all cases simply **1a**, and not (for instance) an adduct in which SbF_6^- has been displaced by CD_2Cl_2.[15]

Qualitatively similar results are seen for BF_4^- adduct **2**, for which observed and calculated spectra are shown in Figure 3 over the temperature range ~190 to 250 K, and in Figure 4 at ~260 to 340 K. Here, the doublet is broader at the lowest temperature examined, so the rate of exchange is expected to be faster than that in **1a** at that temperature, and since only *four* fluorine atoms exchange into the bridging site, a *quintet* is observed in the intramolecular fast exchange limit. The high-temperature spectra are qualitatively similar to those of **1a**, and so similar exchange rates will be expected. For PF_6^- adduct **3**, the intermolecular exchange process yields spectra comparable to those of **1a** and **2**, while the low-temperature intramolecular exchange process is much faster (Figure 5); here a broad doublet is observed at just above the freezing point of CD_2Cl_2 (~162 K in a ~0.1 M sample), and a sharp septet is observed at ~220 K.[16] The ^{31}P NMR spectra of **3** also exhibit signals due to the bound PF_6^- phosph*ate* multiplet (Figure 6). The spectra are always complicated by the presence of free PF_6^- ion of undetermined origin,[13b] but since no phosph*ine singlet* that might be due to the free $Me_3P(CO)_3(NO)W^+$ ion or (more likely) its 18-electron CD_2Cl_2 adduct is observed, there is no evidence that this indicates the presence of

(15) (a) Beck, W.; Schloter, K. *Z. Naturforsch., B* **1978**, *33B*, 1214–1222. (b) Sünkel, K.; Urban, G.; Beck, W. *J. Organomet. Chem.* **1983**, *252*, 187–194. (c) Fernández, J. M.; Gladysz, J. A. *Inorg. Chem.* **1986**, *25*, 2672–2674. (d) Winter, C. H.; Arif, A. M.; Gladysz, J. A. *J. Am. Chem. Soc.* **1987**, *109*, 7560–7561. (e) Colsman, M. R.; Noirot, M. D.; Miller, M. M.; Anderson, O. P.; Strauss, S. H. *Ibid.* **1988**, *110*, 6886–6888. (f) Fernández, J. M.; Gladysz, J. A. *Organometallics* **1989**, *8*, 207–219. **Note Added in Proof**: Structural characterization of a compound that exhibits methylene chloride coordination to Ag^+ has recently been reported: Newbound, T. D.; Colsman, M. R.; Miller, M. M.; Wulfsberg, G. P.; Anderson, O. P.; Strauss, S. H. *J. Am. Chem. Soc.* **1989**, *111*, 3762–3764.

(16) The doublet at −16.6 to −17.2 ppm in Figure 5 is reproducibly observed in the spectra of **3**, and is tentatively thought to be *mer*-(*cis*-Me_3P)-$(CO)_3(NO)WF$.[13b]

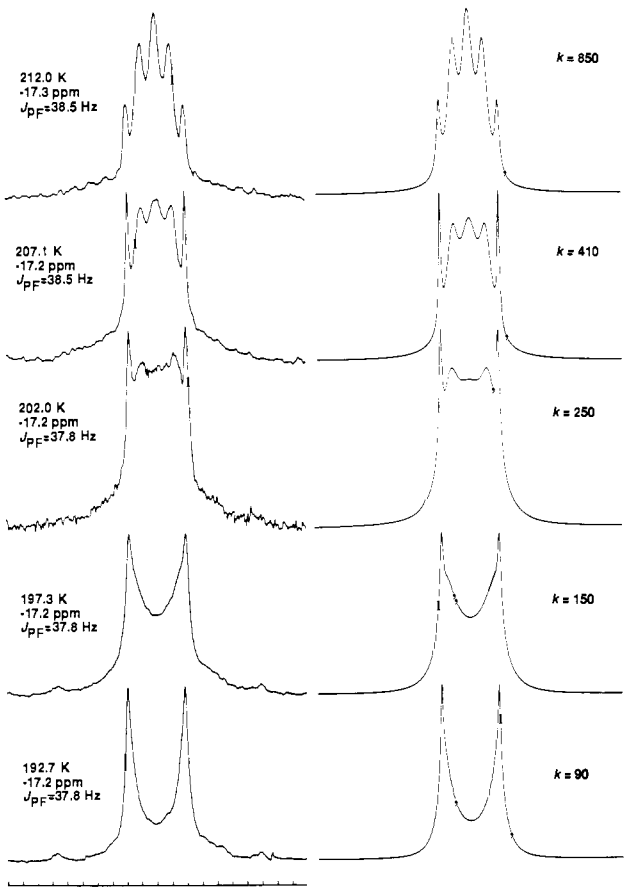

Figure 3. Variable-temperature ^{31}P NMR spectra of **2** on the left (scale markings are at 10-Hz intervals) and best-fit theoretical spectra (rate constants in s^{-1} for the ionic spinning mechanism) on the right, for intramolecular anion exchange.

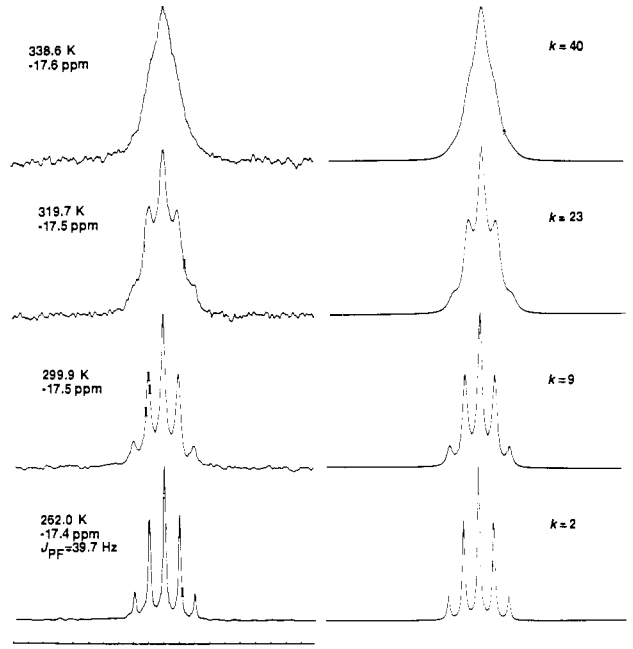

Figure 4. Variable-temperature ^{31}P NMR spectra of **2** on the left (scale markings are at 10-Hz intervals) and best-fit theoretical spectra (rate constants in s^{-1}) on the right, for intermolecular anion exchange.

stable contact or solvent-separated ion pairs arising from **3**. Nevertheless, the spectra are unique in that at low temperature, approach to the slow-exchange limit allows observation of different one-bond coupling constants between the phosphate phosphorus atom and the terminal and bridging fluorine atoms. The equatorial

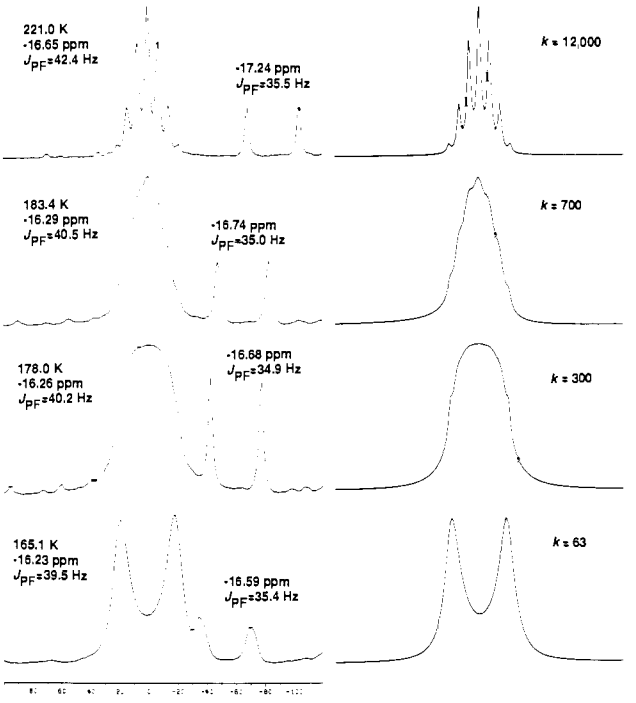

Figure 5. Variable-temperature ^{31}P NMR spectra of **3** (phosphine region only) on the left (scale markings in Hz) and best-fit theoretical spectra (rate constants in s^{-1} for the ionic spinning mechanism) on the right, for intramolecular anion exchange. The doublet at −16.6 to −17.2 ppm is an unidentified impurity.[16]

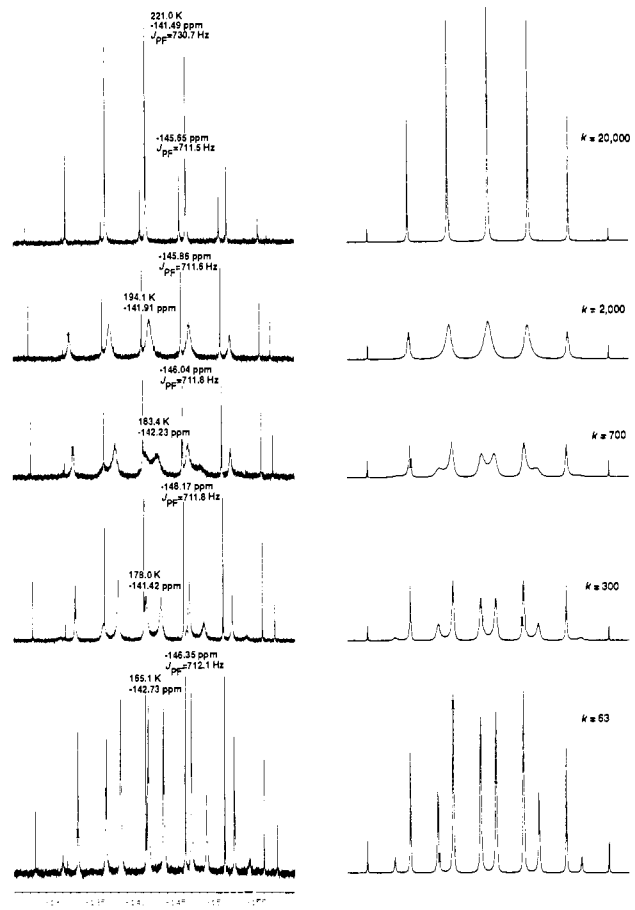

Figure 6. Variable-temperature ^{31}P NMR spectra of **3** (phosphate region only) on the left (scale markings in ppm) and best-fit theoretical spectra (rate constants in s^{-1} for the ionic spinning mechanism) on the right, for intramolecular anion exchange. Free PF_6^- appears as the sharp septet (of which the highest field line is not shown) centered on ca. −146 ppm,[13b] while bound PF_6^- appears as the multiplets centered on ca. −142 ppm.

and axial P–F coupling constants are not resolved, yielding the observed somewhat distorted doublet of sextets; in the fast-exchange limit, the apparent coupling constant $^1J_{PF}$ = 731 Hz in which all six fluorine atoms are "equivalent" is simply the weighted average of the three bridging, equatorial, and axial coupling constants. In the calculated spectra shown in Figure 6, these three coupling constants were taken directly from the well-resolved signals in the ^{19}F NMR spectrum of **3** due to the bridging ($^1J_{P(\mu\text{-}F)}$ = 497 Hz), equatorial ($^1J_{PF}$ = 780 Hz), and axial ($^1J_{PF}$ = 764 Hz) fluorine atoms.[13b] The observed line-spacings in the 165 K spectrum in Figure 6 of 502 ± 3 Hz (for $^1J_{P(\mu\text{-}F)}$) and 776 ± 2 Hz (the weighted average of the four equatorial and one axial coupling constants is 776.8 Hz) are in good agreement.

Line-Shape Analysis. As can be seen by inspection of Figures 1–6, good agreement between observed and calculated NMR line shapes can be obtained, and so the proposed exchange mechanisms that give rise to those theoretical spectra are clearly consistent with experiment. We describe in some detail now how these line shapes arise, in particular, to understand the sharp outermost lines seen in Figures 3 and 6, and to consider whether line shapes alone will allow the intramolecular exchange mechanisms in Scheme III to be distinguished. In the discussion that follows, each "exchange event" is defined in Scheme III and occurs with a rate constant k_{ionic}, $k_{concerted}$, or $k_{dissociation}$; it is important to recognize that an individual exchange event will *not* necessarily result in any spin exchange at the bridging site.

We start by considering **1a**. Each fluorine atom of the SbF_6^- ligand will have an α or β spin. There will be 2^6 = 64 different combinations of spins, in which 1/64 of the anion population will be α^6 (i.e., an SbF_6^- ion in which all six fluorine atoms are in the α spin state), 1/64 will be β^6, 6/64 will be $\alpha\beta^5$, 6/64 will be $\alpha^5\beta$, 15/64 each will be $\alpha^2\beta^4$ and $\alpha^4\beta^2$, and 20/64 will be $\alpha^3\beta^3$. Overall, half of the bridging fluorine atoms will be in the α spin state and half in the β spin state, and so in the slow-exchange limit for the intramolecular process a doublet results.

In the fast-exchange limit, we start by considering the anions that are in the α^6 or β^6 spin states. Exchange will *not* change the spin state of the fluorine atom in the bridging site, so the two outermost lines that arise from these two populations (each accounting for only 1/64 of the intensity of the final spectrum) *do not broaden or change in any way*. This accounts for the appearance of Figure 3, where the α^4 and β^4 spin states of the BF_4^- ion each accounts for *1/16* of the intensity of the final spectrum, and so these lines are quite pronounced since they are four times as intense (relative to the remaining broad lines) as those in **1a**. In a similar manner, the two outermost lines of the bound PF_6^- ligand of **3** are sharp as seen *in* Figure 6, since these lines also arise from the α^6 and β^6 spin states, and so do not change as each of the fluorine atoms exchanges into the bridging, equatorial, and axial sites.

In order to continue discussion of the fast-exchange limit, we must consider the exchange consequences of the two different mechanisms in Scheme III. The simpler scheme is the ionic mechanism, in which an exchange event (that *is*, ionization to contact ion pairs) allows reattachment of any of the six fluorine atoms to tungsten. Consider anions in the $\alpha^3\beta^3$ spin state; since there is an *equal* probability of coordination of a fluorine atom in either spin state, in the fast exchange limit a line will be observed in the NMR at $\nu \pm (J/2)[(3/6) - (3/6)] = \nu$, that is, at the midpoint of the two outermost lines. For anions in the $\alpha^2\beta^4$ and $\alpha^4\beta^2$ spin states, the lines in the fast exchange limit will be observed at $\nu \pm (J/2)[(4/6) - (2/6)] = \nu \pm (J/6)$, and for anions in the $\alpha^1\beta^5$ and $\alpha^5\beta^1$ spin states, the lines in the fast exchange limit will be observed at $\nu \pm (J/2)[(5/6) - (1/6)] = \nu \pm (J/3)$, thereby generating the exchanging five lines of the septet. It should be pointed out that the distance between the two outermost lines, which remains essentially unchanged apart from a small increase with increasing temperature, is the coupling constant J, while the distance between each line of the septet will be $J/6$.

Exchange in the concerted process is illustrated and compared to the ionic process in Scheme IV, where we take as an example the $\alpha^5\beta^1$ spin state in which the bridging fluorine atom is in the

Scheme IV

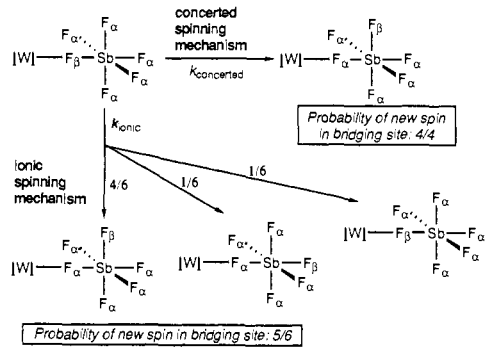

β spin state. An exchange event via the chelate mechanism necessarily places one of the equatorial (α) fluorine atoms in the bridging site, so the exchange event will always be detected at phosphorus; that is, there is a 4/4 probability that an α spin will exchange into the bridging site. In the ionic mechanism, an exchange event is considered to be ion-pair formation, with all six fluorines becoming equivalent; upon recombination, therefore, there is only a 5/6 probability that an α spin will be in the bridging site, with a 1/6 probability that no change will occur due to the β spin reoccupying the bridging site.[17] The exchange matrices for the two mechanisms are obviously different, so different rates and line shapes might be expected. In fact, only different rates result: while in the chelate mechanism a new atom (and hence, potentially, spin) *always* moves into the bridging site in each exchange event, in the ionic mechanism there is *only a 5/6 chance that a new spin moves into the bridging site*. To yield the same degree of spin exchange (and hence broadening), the rate of exchange in the chelate mechanism would only have to be 5/6 the rate of the ionic mechanism. In practice, when we *set* the exchange rate in the chelate mechanism equal to 5/6 that of the ionic mechanism, *the line shapes are indistinguishable*. For this reason, all rate constants quoted in this paper will be the ionic rate constants, since the concerted rate constants are readily derived from them. For the tetrahedral anion BF_4^-, the situation is slightly different, since there is no distinction between the three terminal fluorine atoms of adduct **2** in a manner analogous to the equatorial and axial fluorine atoms of **1** and **3**. Apart from the fact that there is only a 3/4 chance of bridging atom exchange for each exchange event in the ionic mechanism while there is a 3/3 chance in the chelate mechanism, the exchange matrices are *identical* for the two mechanisms for **2**, so the line shapes are rigorously identical for $k_{concerted} = (3/4)k_{ionic}$.

The line-shape analysis for the intermolecular process is relatively straightforward. The septet or quintet is set as the *slow* exchange limit by assigning the appropriate relative intensities to each line, and then allowing population-weighted exchange of each line with all others with a rate constant $k_{dissociation}$. Details of each of the exchange matrices used in Figures 1–6 may be found in the Experimental Section.

Analysis of the Data. Methylene Chloride Solvent. The rate data for the low-temperature intramolecular exchange process is collected in Table I, where as noted above the rate constants assume the ionic mechanism, and the data for the high temperature intermolecular exchange process is collected in Table II. The activation parameters are derived from Eyring plots of ln (k/T) versus T^{-1}, and error limits were determined as described in the Experimental Section. In the case of the concerted mechanism, where $k_{concerted} = (5/6)k_{ionic}$ or $(3/4)k_{ionic}$ for **1** and **3**, and **2**, respectively, only $\Delta S^{\ddagger}$ changes, by R ln (5/6) = –0.36 eu for the 5/6 factor and by R ln (3/4) = –0.57 eu for the 3/4 factor. Such differences are experimentally indistinguishable, and in the following discussion only the ionic values will be considered for the activation parameters as well as the rates.

(17) The 4:1 equatorial:axial probability for location of the β spin, shown for completeness in Scheme IV, has no effect since this information is lost upon reionization.

Table I. Rate Data for Intramolecular Anion Exchange

entry	compd	solvent[a]	conc (M)	temperature (K)/rate constant[b] (s^{-1})										$\Delta H^{\ddagger}$[c]	$\Delta S^{\ddagger}$[c]	$\Delta G^{\ddagger}$[c]
I.1	**1a**	CD_2Cl_2	0.057	193.7	198.6		205.5	210.4	215.6	222.4	227.1	232.3	241.2	250.1	9.96 ± 0.24	−1.52 ± 1.10	10.35 ± 0.38
				9	22		60	105	190	340	490	860	2100	5400			
I.2	**1a**	CD_2Cl_2	0.020	193.2				209.9	215.1	221.3		231.4		266.0[d]	8.87 ± 0.28	−6.11 ± 1.31	10.46 ± 0.44
				16				125	220	350		875		5000			
I.3	**1a**	CD_2Cl_2/CS_2	0.057	194.2				209.9	215.1	221.3		230.9			9.44 ± 0.34	−3.82 ± 1.59	10.43 ± 0.54
				13				107	180	300		775					
I.4	**1b**	CD_2Cl_2	0.074	193.7		202.0		209.9	215.1	221.3		230.9	238.2	247.3	7.05 ± 0.32	−15.88 ± 1.48	11.18 ± 0.50
				19		35		55	90	150		350	600	1200			
I.5	**1b**	hexane/CD_2Cl_2	0.074	193.7				209.9	215.1	221.3		230.0		247.8	7.11 ± 0.42	−15.50 ± 1.91	11.14 ± 0.65
				19				60	90	180		400		1200			
I.6	**1b**	hexane	0.076	193.7		201.5		211.9		220.8		230.9	238.7	247.8	5.56 ± 0.45	−22.52 ± 2.06	11.41 ± 0.70
				35		45		70		150		350	500	900			
I.7	**1b**	hexane	0.0038	193.7						220.8				247.8	5.39 ± 1.22	−23.15 ± 5.63	11.41 ± 1.91
				35						125				1000			
I.8	**2**	CD_2Cl_2	0.047	192.7	197.3	202.0	207.1	212.0		221.7				251.0[d]	8.11 ± 0.44	−6.61 ± 2.13	9.83 ± 0.71
				90	150	250	410	850		1500				8000			
I.9	**2**	CD_2Cl_2/CS_2	0.025	192.1	196.3	201.0	205.7	210.9		220.8					8.20 ± 0.09	−6.50 ± 0.46	9.89 ± 0.15
				70	120	190	310	525		1350							
I.10	**3**	CD_2Cl_2	0.13	165.1	168.3	172.6	178.0	183.4	194.1	204.9	221.0				6.31 ± 0.22	−10.74 ± 1.22	9.10 ± 0.39
				63	107	145	300	700	1550	3000	12000						

[a] CD_2Cl_2/CS_2 is 90:10 v/v; hexane:CD_2Cl_2 is 71:29 v/v. [b] Rate constants are k_{ionic} (Scheme III); $k_{concerted} = (5/6)k_{ionic}$. [c] Activation parameters in kcal/mol ($\Delta G^{\ddagger}$, $\Delta H^{\ddagger}$) and eu ($\Delta S^{\ddagger}$); determined from Eyring plots; $\Delta G^{\ddagger}$ calculated at 260 K. [d] Not used in Eyring plot.

Table II. Rate Data for Intermolecular Anion Exchange

entry	compd	solvent[a]	conc (M)	temperature (K)/rate constant[b] (s^{-1})						$\Delta H^{\ddagger}$[c]	$\Delta S^{\ddagger}$[c]	$\Delta G^{\ddagger}$[c]
II.1	**1a**	CD_2Cl_2	0.057	267.4	286.0	305.9		323.7	343.5	6.63 ± 0.35	−30.69 ± 1.16	14.60 ± 0.46
				4.0	10	25		50	75			
II.2	**1a**	CD_2Cl_2/CS_2	0.057	266.1	284.5	305.5	314.8	324.1	343.5	6.50 ± 0.28	−31.32 ± 0.91	14.64 ± 0.36
				4.0	8	18	30	40	80			
II.3	**1b**	CD_2Cl_2	0.074	266.1	284.5	305.1		323.7	333.8	4.22 ± 0.71	−39.91 ± 2.39	14.59 ± 0.95
				4.5	5	10		20	25			
II.4	**1b**	hexane/CD_2Cl_2	0.074	265.6	284.9	305.5		324.1	343.5	4.81 ± 0.48	−37.30 ± 1.59	14.51 ± 0.63
				5	7	15		30	45			
II.5	**1b**	hexane	0.076	266.1	284.5	304.3		323.4		5.19 ± 0.73	−35.20 ± 2.51	14.34 ± 0.98
				7	10	25		45				
II.6	**1b**	hexane	0.0038	266.1	284.5	304.3		323.4		2.16 ± 0.45	−46.79 ± 1.52	14.33 ± 0.60
				6	7	10		15				
II.7	**2**	CD_2Cl_2	0.041	262.0	280.5	299.9		319.7	338.6	6.39 ± 0.27	−32.61 ± 0.92	14.87 ± 0.36
				2	4.5	9		23	40			
II.8	**2**	CD_2Cl_2/CS_2	0.025	260.1	279.3	299.5		319.3	338.6	5.42 ± 0.98	−36.27 ± 3.30	14.85 ± 1.30
				2.5	3.0	6.0		15	35			
II.9	**3**	CD_2Cl_2	0.034	231.8[d]	261.1	290.2	312.4			4.70 ± 1.87	−36.67 ± 6.56	14.23 ± 2.53
				4	7	12	40					

[a] CD_2Cl_2/CS_2 is 90:10 v/v; hexane:CD_2Cl_2 is 71:29 v/v. [b] Rate constants are $k_{dissociation}$ (Scheme III). [c] Activation parameters in kcal/mol ($\Delta G^{\ddagger}$, $\Delta H^{\ddagger}$) and eu ($\Delta S^{\ddagger}$); determined from Eyring plots; $\Delta G^{\ddagger}$ calculated at 260 K. [d] Not used in Eyring plot.

The intramolecular exchange process for **1a** in methylene chloride (entry I.1) has $\Delta H^{\ddagger} \approx 10$ kcal/mol, and $\Delta S^{\ddagger} \approx 0$ eu, while the intermolecular process (entry II.1) has $\Delta H^{\ddagger} \approx 6.6$ kcal/mol and $\Delta S^{\ddagger} \approx -31$ eu. Thus, the high-temperature exchange process has a *lower* activation enthalpy, but because of the remarkably negative activation entropy the overall free energy of activation is ~4 kcal/mol higher at 260 K. The obvious interpretation of the intermolecular activation entropy is that solvation of the transition state leading to the free ions is much greater than the solvation of the covalent adduct **1a**, which is a perfectly reasonable hypothesis; it is important to keep in mind that all activation parameters are measured with respect to the ground-state adduct. Interpretation of the intramolecular activation entropy is mechanism dependent. One might expect a negative activation entropy for the concerted mechanism due to restriction of the motion of the anion in the chelate transition state illustrated in Scheme III, but since the exchange would be unimolecular and not invole any loss of translational freedom, the effect would be small.[18] For the ionic mechanism (Scheme III) one would balance the positive contribution arising from formation of two particles from one, with the negative contribution arising from increased solvation. The magnitude of the *inter*molecular activation entropy suggests that the solvation effect should dominate. Thus, such an analysis might favor the chelate mechanism. However, the lower activation enthalpy for the high-temperature exchange is, at least on an intuitive level, inconsistent with the chelate mechanism. That is, one would expect the chelate mechanism to have a relatively *low* activation enthalpy, since the bond cleavage ought to be balanced by bond formation in the transition state; a subsequent *lower* activation enthalpy for complete bond cleavage to the free ions seems unreasonable. Nonetheless, such expectations cannot rigorously hold, since the observed enthalpies are *not* bond energies, but reflect significant degrees of solvation. We will return to these points later; as will be seen in the discussion of results that follows, the above observations will develop into a trend.

The next data point demonstrates that the intramolecular exchange process is unimolecular. Spectra were taken for **1a** at approximately one-third the concentration initially examined, and inspection of the rate constants (entry I.2) demonstrates that they are essentially the same for the two runs. The constancy of $\Delta G^{\ddagger}$ is not unexpected, given the reasonably large temperature ranges covered (~40–60 °C), but as seen $\Delta H^{\ddagger}$ and $\Delta S^{\ddagger}$ are not the same but do compensate for one another. We suspect that this result is a consequence of experimental error,[19] but we will return to this point later.

The rate constants for intramolecular exchange for BF_4^- adduct **2** in methylene chloride (entry I.8) are substantially greater than those for **1a**, ~10 times greater at ~193 K and ~5 times greater

(18) Schalegar, L. L.; Long, F. A. *Adv. Phys. Org. Chem.* **1963**, *1*, 1–33.

(19) Sandström, J. *Dynamic NMR Spectroscopy*; Academic Press: New York, 1982; Chapter 7.

at 222 K. As a result, both $\Delta G^{\ddagger}$ (~9.8 kcal/mol) and $\Delta H^{\ddagger}$ (~8 kcal/mol) are significantly smaller (implying a weaker W–F bond, all other factors being equal), which is consistent with the ionic mechanism when one considers that the BF_4^- adduct is less stable than the SbF_6^- adduct.[13b] Most significantly, the high temperature parameters (entry II.7) are essentially the same as those of **1a**, with $\Delta H^{\ddagger} \approx 6.4$ kcal/mol and $\Delta S^{\ddagger} \approx -33$ eu. Given the difference in stabilities of **1a** and **2**, the similarity of their intermolecular exchange rates strongly suggests that this process does *not* involve bond cleavage as would be required by the chelate mechanism, but is simply due to diffusion of the ions apart to give the free ions, a process that could reasonably give similar parameters for different ions.

The intramolecular exchange rate constants for PF_6^- adduct **3** (entry I.10) were determined with a high degree of confidence, since the line-shape analyses of *both* the PMe_3 and PF_6^- regions of the spectrum yield similar rates of exchange. The lowest temperature rate constants are in precise agreement, while at the higher temperatures the PF_6^- region yields higher rate constants; since the line widths in the absence of exchange (i.e., T_2) are taken from $Me_3PW(CO)_5$, the rate constants from the PMe_3 region are likely to be more accurate.[19] The exchange rate constants (entry II.9) are *much* faster than those measured for **1a** and **2**; for instance, rates at ~190 K are ~10 s^{-1} for **1a**, ~90 s^{-1} for **2**, and ~1500 s^{-1} for **3**. In sharp contrast, the rate constants for the high-temperature exchange reaction are essentially the same as those of **1a** and **2**, even though the data are not as accurate since some decomposition of this least thermally stable adduct is evident; derived parameters are $\Delta H^{\ddagger} \approx 5 \pm 2$ kcal/mol and $\Delta S^{\ddagger} \approx -37 \pm 7$ eu. Hence, since **3** is much less stable than **1a** and **2**, the conclusion is even more strongly drawn that bond cleavage occurs in the low-temperature exchange and diffusion out of the solvent cage occurs in the high-temperature exchange.

We briefly examined whether this low-temperature *kinetic* barrier would be reflected in any *thermodynamic* preference of the tungsten cation for SbF_6^- over PF_6^-, according to eq 1. Thus,

$$\mathbf{1a} + PF_6^- \rightleftarrows \mathbf{3} + SbF_6^- \quad (1)$$

1.14 equiv of $(Ph_3P)_2N^+PF_6^-$ was added to **1a** and the mixture examined by ^{31}P NMR. At 299.4 K and at 178.0 K, the observed ratio of **3**:**1a** was 68 ± 1:32 ± 1; a plot of ln K for eq 1 versus T^{-1} for the two temperatures gives $\Delta H^{\circ} \approx 0.1$ kcal/mol and $\Delta S^{\circ} \approx 2$ eu.[20] Given the apparently greater stability of **1a** relative to **3**, this result stands in contrast to what we would have expected. However, the equilibrium necessarily involves the $(Ph_3P)_2N^+$ ion *pairs*, not the free ions shown, and these will not necessarily be isoenergetic for the two anions. That is, the stability of the ion pair with SbF_6^- could be greater than with PF_6^-, balancing any effect due to greater stability of **1a** over **3**. Nonetheless, it has been reported that association constants for $(Ph_3P)_2N^+$ salts of more coordinating anions are essentially constant ($K_A = 1\text{–}2 \times 10^3$ in CH_2Cl_2 at 25.00 °C), and claimed that ratios such as that of **3**:**1a** are truly independent of effects due to the $(Ph_3P)_2N^+$ ion.[11a] We conclude that the differences are likely to be slight, given that ΔG° here is ~0.4 kcal and that the kinetic barrier $\Delta\Delta G^{\ddagger}$ is ~1.3 kcal at 260 K, albeit in the opposite sense; we have not yet made any attempt to further examine this equilibrium.

Other Solvents: Carbon Disulfide and Hexane. The most direct means by which to distinguish the concerted and ionic mechanisms would involve the dependence of reaction rates on solvent polarity. Clearly, in more polar solvents one would expect to lower the barrier to ionization, so if the concerted mechanism is correct, the *high*-temperature process would be faster, while if the ionic mechanism is correct, the *low*-temperature process would be faster.[6b] Unfortunately, we have not found a solvent more polar than methylene chloride (dielectric constant[21] $\epsilon = 8.9$) that does not prevent internal return of the contact ion pair; in terms of Scheme I, such solvents give rise exclusively to the analogue of hydrolysis, namely, displacement of the "noncoordinating" anions. Solvents examined[22] include acetone ($\epsilon = 20.7$), ethanol ($\epsilon = 24.3$), trifluoroethanol ($\epsilon = 26.5$), acetonitrile ($\epsilon = 36.2$), dimethylformamide ($\epsilon = 36.7$), dimethyl sulfate ($\epsilon = 42.6$), and dimethyl sulfone (a solid analogue for sulfolane, $\epsilon = 44$). However, a *less* polar solvent, carbon disulfide ($\epsilon = 2.64$), was found *not* to displace the "noncoordinating" anions, so this was examined next; here the predictions would be opposite those noted above. Unfortunately, the solubility of **1a** and **2** was not high in CS_2, so two runs were conducted in 90:10 CD_2Cl_2/CS_2 ($\epsilon = 8.3$; entries I.3, I.9, II.2, II.8). Since at this concentration of CS_2 the solvent polarities were essentially the same, our expectation was that these runs should simply corroborate the data previously obtained in pure CD_2Cl_2, and this was, in fact, observed. For both **1a** and **2** the two sets of activation parameters for both exchange reactions were indistinguishable.

In order to present the largest difference in polarity feasible, we sought next to use hexane ($\epsilon = 1.89$) as a reaction solvent. While the Me_3P-containing SbF_6^- adduct **1a** was insoluble as expected, the tri*octyl*phosphine adduct **1b** was quite soluble in hexane. Our specific predictions here were that little change in intramolecular rates would be expected for the concerted mechanism, while a significant drop in rates would be expected given the ionic mechanism. Furthermore, we did not anticipate that the high-temperature *inter*molecular exchange would occur at all, since formation of free ions in hexane did not seem reasonable. Hence the observed high-temperature *intermolecular* exchange (entry II.5) was extraordinarily surprising; not only did it occur, but if anything $\Delta G^{\ddagger}$ was marginally *lower* than that seen for **1a** (and **1b**) in methylene chloride. The other high-temperature activation parameters were also similar, with $\Delta H^{\ddagger} \approx 5.2 \pm 0.7$ kcal/mol and $\Delta S^{\ddagger} \approx -35 \pm 3$ eu. The low-temperature exchange parameters (entry I.6) of $\Delta H^{\ddagger} \approx 5.6 \pm 0.5$ kcal/mol and $\Delta S^{\ddagger} \approx -23 \pm 2$ eu were, in fact, quite similar, and we are tempted to argue that if the former set necessarily represents an ionic process, then the latter set ought to as well. Nevertheless, another possibility made reasonable by the −35 eu entropy was that the high-temperature exchange process was *bimolecular* and did *not* involve free ions; one can imagine a process in which two molecules of **1b** interact and effect a concerted exchange of anions. Thus, the activation parameters were measured at *one-twentieth* of the initial concentration of **1b** used. The rate constants at low temperature (entry I.7) were virtually the same as before; only three temperatures were used so the deviations of the activation parameters are large. For the high-temperature exchange (entry II.6), the rate constants are noticeably lower; this is evident as well by direct inspection of the spectra themselves, in which (for instance) the signal in the high-concentration spectrum is above the coalescence temperature at 304 K, while in the low-concentration spectrum fine structure is clearly visible. Nevertheless, a bimolecular reaction would have resulted in a 20-fold reduction in rate, so since the rate constants are essentially the same at 266 K and diverge by only a factor of 3 by 323 K, the reaction is clearly *not* bimolecular. Both high- and low-concentration Eyring plots are linear, and the low concentration parameters of $\Delta H^{\ddagger} \approx 2.2 \pm 0.5$ kcal/mol and $\Delta S^{\ddagger} \approx -47 \pm 2$ eu are even more surprising. It should be noted that a complication arises from the experimental method. Since **1b** is an oil, it is impossible to be certain that all the methylene chloride solvent used in its preparation is removed by evacuation. Analysis of both hexane samples by ^1H NMR shows that the high-concentration sample contains ≤0.7 mol % of CH_2Cl_2 in C_6H_{14}, which corresponds, however, to a concentration of 0.05 M, or nearly 1 equiv of methylene chloride. The low-concentration sample has no detectable CH_2Cl_2, but while our detection limit is only <0.008 M, there is no reason to suppose that the CH_2Cl_2 is not diluted to the same extent as **1b**. Nev-

(20) The spectra are also complicated by the presence of the doublet impurity noted above,[16] as well as an adduct with (perhaps) water; the primary conclusion is not affected if as seems reasonable any additional ion pairs do not differ substantially in stability, in a manner as explained below analogous to the $(Ph_3P)_2N^+$ ion pairs.[11a]

(21) Gordon, A. J.; Ford, R. A. *The Chemist's Companion*; Wiley: New York, 1972; pp 3–13.

(22) Honeychuck, R. V; Hersh, W. H. *Inorg. Chem.* **1987**, *26*, 1826–1828.

ertheless, if methylene chloride has any specific solvating effect, one might expect the low-concentration parameters to better reflect the effect of the nonpolar solvent on the reaction rates, and we will assume that the data accurately reflect ionization in hexane.

Lastly, given the fast that **1b** has a considerably bulkier phosphine ligand than **1a** (the cone angle[23] of Me_3P is 118° while that of $(n\text{-octyl})_3P$ is effectively ≥ 140–145°[24]), it was imperative to examine the exchange rates of **1b** in methylene chloride for comparison. The intramolecular exchange parameters (entry I.4) were closer to those of **1b** in hexane (entry I.6) than to those of **1a** in methylene chloride (entry I.1), with $\Delta H^{\ddagger} \approx 7.1 \pm 0.3$ kcal/mol and $\Delta S^{\ddagger} \approx -16 \pm 1$ eu. The intermolecular exchange rate constants (entry II.3) were lower overall and yielded somewhat different activation parameters from **1a** ($\Delta H^{\ddagger} \approx 4.2 \pm 0.7$ kcal/mol and $\Delta S^{\ddagger} \approx -40 \pm 2$ eu), and a run using a 29:71 ratio of methylene chloride/hexane (entry II.4) yielded $\Delta H^{\ddagger} \approx 4.8 \pm 0.5$ kcal/mol and $\Delta S^{\ddagger} \approx -37 \pm 2$ eu, values that are intermediate between those of **1b** in methylene chloride and hexane. Nevertheless, the most conservative conclusion is that the high-temperature exchange process for **1b** is relatively *insensitive* to solvent; from the average of the three high-concentration runs (entries II.3–5), we obtain $\Delta H^{\ddagger} \approx 4.7 \pm 0.4$ kcal/mol and $\Delta S^{\ddagger} \approx -37 \pm 2$ eu, values that are somewhat different from those of the less bulky **1a** ($\Delta H^{\ddagger} \approx 6.6$ kcal/mol and $\Delta S^{\ddagger} \approx -31$ eu). Lastly, we note that the rate constants for intramolecular exchange for **1b** in the 29:71 methylene chloride/hexane solvent (entry I.5) were the same as those in methylene chloride rather than being intermediate between the methylene chloride and hexane values, so the initial ionization to the proposed ion-pair intermediate seems to be sensitive to the presence of methylene chloride. While the intramolecular exchange parameters are clearly different for the bulkier compound, and the intermolecular parameters are probably different, they once again provide support for the ionic mechanism: the activation enthalpy is higher and the activation entropy is substantially negative for the low-temperature process, implying bond cleavage and a well-solvated transition state.

Discussion

We now consider in detail how the trends in the activation parameters themselves may serve to define the mechanisms of the two exchange processes. That is, is the low-temperature intramolecular exchange process concerted or ionic as defined in Scheme III, how do the anion, ligand bulk, and solvent polarity affect the transition state energies, and does the high-temperature intermolecular exchange process really involve free ions in hexane?

Ionic versus Concerted Intramolecular Exchange. Four key points may be made. First, the relative order of intramolecular $\Delta G^{\ddagger}$ (and $\Delta H^{\ddagger}$) as a function of anionic ligand is **1a > 2 > 3**, which is the same order of the stability of these compounds and of the coordinating ability of the anions SbF_6^-, BF_4^-, and PF_6^- which was previously determined on the basis of solid-state structures.[13b] Such a result is completely consistent with bond *cleavage* in the transition state leading to ionization, while it is unclear what trend might be expected in the chelate transition state of the concerted mechanism since bond *formation* also occurs. We note also that the stability of these compounds must be a *kinetic* phenomenon (that is, the barrier to decomposition follows the order **1a > 2 > 3**), since there is no ground-state *thermodynamic* preference for coordination of SbF_6^- as seen in the equilibrium experiment with $(Ph_3P)_2N^+PF_6^-$. Second, for a given set of compound, concentration, and solvent, the intramolecular $\Delta H^{\ddagger}$ is greater than the intermolecular $\Delta H^{\ddagger}$ *in every case*. This too is consistent with bond cleavage in the former but not latter step, as occurs in the ionic but not concerted mechanism. Third, all of the activation parameters are remarkably similar for the intermolecular process; with the exception of the low concentration data point in hexane (entry II.6), $\Delta H^{\ddagger}$ averages 5.5 ± 0.9 kcal/mol, and $\Delta S^{\ddagger}$ averages −35 ± 3 eu. This suggests that bond cleavage is *not* likely in this step, but diffusion of the ions out of a solvent cage could reasonably yield similar activation parameters for a variety of reasonably similar ions. Lastly, the high-temperature intermolecular exchange seemingly *must* involve relatively free ions. which according to Scheme I must be preceded by an ion pair. Therefore, the most simple hypothesis is that this necessary ion pair must give rise to the observable intramolecular process, since in the absence of compelling data the concerted process is an additional and unnecessary complication.

Structure of the Ion Pair. In order to facilitate the discussion that follows, we now explicitly consider the structure of the ion pair. The formation of the ion pair in hexane at rates comparable to those seen in methylene chloride, while at odds with expectation, suggests that the ion pair is not particularly ionic, and that no special stabilization of the transition state by a polar solvent is required. This is, of course, what the concerted mechanism would predict, but the apparent observation, on the basis of the high-temperature exchange process, of free ions in hexane as well tends to mitigate the validity of that prediction. A plausible "ion-pair" structure is that shown by **4**, in which W–F bond cleavage has

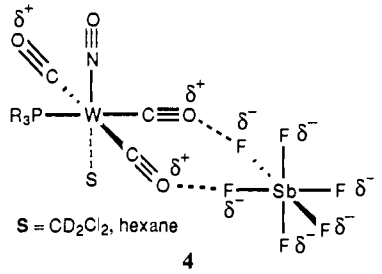

4

occurred, but in which the two ions are, nevertheless, still bound and hence the "pair" is fairly nonionic in nature. While ion pairing in transition metal carbonyl compounds is normally seen with metal *anions* and alkali metal *cations* via interaction at the negatively charged carbonyl oxygen atoms,[25] here the metal complex is cationic, the nitrosyl ligand is strongly π-acidic, and a partial *positive* charge on the carbonyl oxygen atoms is expected. Consistent with this electrostatic prediction, many short intermolecular oxygen–fluorine contacts are seen in the solid-state structures of these tungsten nitrosyl adducts;[13b] it is for this reason that two contacts are shown in **4**, although this is not necessary. Finally, an obvious question to be raised is whether the observed ion pair is an *unsaturated* 16-electron ion pair or is a *saturated* 18-electron complex with solvent as a sixth ligand. We suggest the latter and so illustrate **4** as the 18-electron ion pair, since methylene chloride has been observed to be a coordinating ligand toward transition metal cations,[15] and *hexane* has been observed to be a coordinating ligand toward neutral metal carbonyls,[26] providing a substantial degree of stabilization for the 16-electron species that might be an intermediate or transition state. While we will return to this thermodynamic point in the section on Energies of the Intermediate Ion Pairs, our data do not directly address the kinetic issue of the mechanism of ionization. That is, do the observed activation parameters arise from a transition state leading to the unsaturated 16-electron complex formed by simple unimolecular ionization of the anion, or from a transition state leading directly to the saturated 18-electron ion pair **4** formed by bimolecular substitution of solvent for the anion? Both dissociative and associative substitution is well known in tungsten carbonyl compounds,[27] but given the similarity in intramolecular rates of exchange for **1b** in methylene chloride and in the much less nucleophilic solvent hexane, the dissociative mechanism ought to be favored here. Even if any methylene chloride present as

(23) Tolman, C. A. *Chem. Rev.* **1977**, *77*, 313–348.
(24) Boyles, M. L.; Brown, D. V.; Drake, D. A.; Hostetler, C. K.; Maves, C. K.; Mosbo, J. A. *Inorg. Chem.* **1985**, *24*, 3126–3131.
(25) See, for instance: (a) Edgell, W. F.; Hegde, S.; Barbetta, A. *J. Am. Chem. Soc.* **1978**, *100*, 1406–1417. (b) Darensbourg, M. Y.; Jimenez, P.; Sackett, J. R.; Hanckel, J. M.; Kump, R. L. *Ibid.* **1982**, *104*, 1521–1530. (c) Darensbourg, M. Y.; Hanckel, J. M. *Organometallics* **1982**, *1*, 82–87. (d) Ash, C. E.; Delord, T.; Simmons, D.; Darensbourg, M. Y. *Ibid.* **1986**, *5*, 17–25.
(26) Simon, J. D.; Peters, K. S. *Chem. Phys. Lett.* **1983**, *98*, 53–56. (b) Yang, G. K.; Peters, K. S.; Vaida, V. *Ibid.* **1986**, *125*, 566–568.
(27) (a) Angelici, R. J. *Organomet. Chem. Rev.* **1968**, *3*, 173–226. (b) Dobson, G. R. *Acc. Chem. Res.* **1976**, *9*, 300–306.

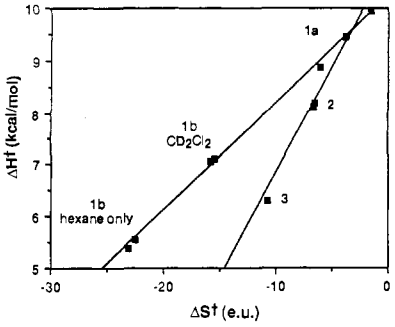

Figure 7. Isokinetic plot of intramolecular exchange activation parameters. The best-fit line to all the data except **3**[30] is nearly indistinguishable from the line for the SbF_6^- series, so only the latter of these two is plotted.

an impurity is the true nucleophile in hexane, its low concentration would be expected to alter the rate of exchange in any bimolecular substitution mechanism, particularly in the runs with **1b** where the concentrations are expected to differ by a factor of 20. Nonetheless, if anion dissociation is rate determining, the barrier between the 16-electron ion pair and the 18-electron ion pair would have to be relatively small and hence the lifetime of the putative 16-electron ion pair could be vanishingly short. One can reasonably imagine a continuum of anion cleavage and front-side solvent participation in the ionization reaction,[9a,28] so the observed activation barriers could simply reflect increased solvation of the ionic compared to neutral (covalent) species, or actual coordination of solvent to directly give **4**.

Isokinetic Analysis of Intramolecular Exchange. In contrast to the high-temperature intermolecular data, the differences in the activation parameters for the low-temperature process clearly imply some type of mechanistic diversity, so the obvious question is whether or not the *same* mechanism can somehow account for each of these intramolecular exchange reactions. The standard means by which to examine this question is to look for an isokinetic relationship (eq 2);[29] while $h°$ has no physical significance, β

$$\Delta H^{\ddagger} = h° + \beta\Delta S^{\ddagger} \quad (2)$$

represents the temperature at which all reactions would proceed at the same rate (hence isokinetic). If a series of related reactions exhibit such a relationship, the mechanism is assumed to be the same for each reaction, with one dominant interaction mechanism responsible for the variation of $\Delta H^{\ddagger}$ with $\Delta S^{\ddagger}$. In fact, a plot of $\Delta H^{\ddagger}$ versus $\Delta S^{\ddagger}$ for the intramolecular exchange parameters yields a reasonably linear plot (aside from the point due to **3**) as seen in Figure 7. The problem, however, is that values of $\Delta H^{\ddagger}$ and $\Delta S^{\ddagger}$ for any individual reaction are *not* independent; they are highly correlated along a line whose slope is equal to the mean temperature of the reactions used to generate the Eyring plot.[29] Thus, observation of the relationship defined by eq 2 is not statistically significant, since if the same temperature range is used to generate each point, a straight line whose slope *is* the mean temperature may result.[30] Nonetheless, Exner has shown[29] that statistically significant evidence for an isokinetic relationship *can* be obtained from the same data, by plotting the logarithms of the rate constants at two temperatures against one another as shown in eq 3; the connection between eq 2 and 3 is given by eq 4. The

$$\log k_2 = a + b \log k_1 \quad (k_2 \text{ is at } T_2,\ k_1 \text{ is at } T_1, \text{ and } T_2 > T_1) \quad (3)$$

$$\beta = T_1T_2(1 - b)/(T_1 - bT_2) \quad (4)$$

key is that *rate constants* are *not* statistically correlated in any way, so observation of a linear plot of the type in eq 3 provides

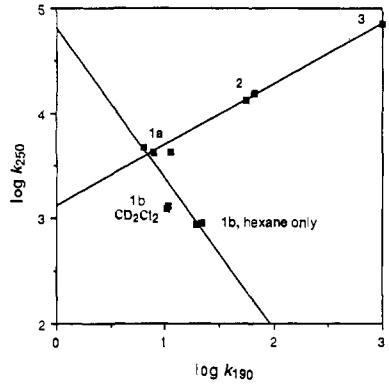

Figure 8. Isokinetic plot of log of the intramolecular exchange rate at 250 K versus that at 190 K. For the PMe_3 series the slope is $b = 0.579 \pm 0.038$, and for the SbF_6^- series $b = -1.433 \pm 0.469$.

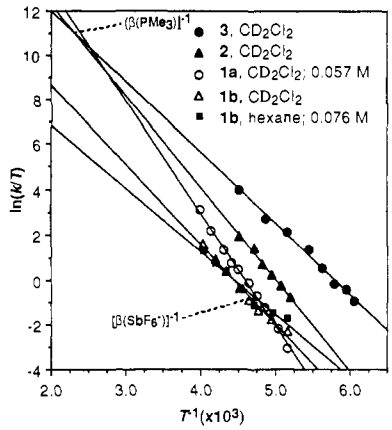

Figure 9. Eyring plots of representative data for each isokinetic series; dashed lines point to the intersection point (β^{-1}, ln (k/β) calculated from lines in Figure 8.

statistically meaningful evidence of an isokinetic relationship. As can be seen in Figure 8, while the intramolecular data clearly do not form *one* isokinetic relationship (hence proving the validity of the above statistical concerns), *two* linear relationships are evident. *One isokinetic relationship is observed for* the *PMe_3 adducts* ***1a***, ***2***, *and* ***3***, *and one isokinetic relationship is observed for the SbF_6^- adducts* ***1a*** *and* ***1b***. Examination of the original plot of $\Delta H^{\ddagger}$ versus $\Delta S^{\ddagger}$ clearly shows these two lines as well, and values of β derived from the statistically different types of plots are in good agreement; from the $\Delta H^{\ddagger}$ versus $\Delta S^{\ddagger}$ plot, $\beta(PMe_3) = 404 \pm 45$ K ($R = 0.976$) and $\beta(SbF_6^-) = 207 \pm 4$ K ($R = 0.999$), while the log–log plot yields (after application of eq 4) $\beta(PMe_3) = 442 \pm 101$ K ($R = 0.992$) and $\beta(SbF_6^-) = 211 \pm 61$ K ($R = 0.807$). Finally, Exner has described in great detail how the least biased means for demonstrating the existence of an isokinetic relationship involves putting all of the Eyring plots on a single graph, and observing whether or not the lines intersect at a single point.[29b] Representative plots are shown in Figure 9 for the two isokinetic series, and provide good support for the isokinetic relationships.

Since the two isokinetic series contain a common member, namely **1a**, the key conclusion from the isokinetic analysis is that one mechanism *can* account for the differences in activation parameters in the low-temperature exchange process. Nonetheless, the observation of a different isokinetic series for each of the two classes of compounds is inherently reasonable, since the isokinetic relationship requires a common cause (that is, a single interaction mechanism) for the correlation of $\Delta H^{\ddagger}$ and $\Delta S^{\ddagger}$. In the PMe_3 group, the anion only (to the extent that the methylene chloride/carbon disulfide system is the same as the methylene chloride solvent) is varied while the degree of steric hindrance is kept constant, while in the SbF_6^- group, both steric hindrance and solvent are varied while the anion is kept constant. We briefly consider the two series in turn.

(28) Reenstra, W. W.; Jencks, W. P. *J. Am. Chem. Soc.* **1979**, *101*, 5780–5791.

(29) (a) Exner, O. *Collect. Czech. Chem. Commun.* **1964**, *29*, 1094–1113. (b) Exner, O. *Progr. Phys. Org. Chem.* **1973**, *10*, 411–482.

(30) Excluding **3**, the slope of the $\Delta H^{\ddagger}$ vs. $\Delta S^{\ddagger}$ plot gives $\beta = 194 \pm 14$ K ($R = 0.981$); the mean reaction temperature is 215.5 K and the mean reaction temperature for the Eyring plot of **3** is 185.9 K.

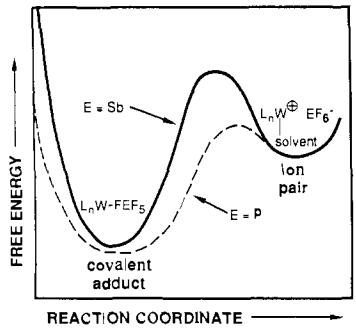

Figure 10. Reaction coordinate diagram for ionization to the ion pair; reaction coordinate for **1a** is the thick solid line and for **3** the dashed line.

In the PMe_3 isokinetic group, $\Delta G^{\ddagger}$ decreases from 10.4 kcal/mol (SbF_6^-) to 9.9 kcal/mol (BF_4^-) to 9.1 kcal/mol (PF_6^-), consistent with our contention that W–F bond cleavage is occurring in this step, since the order of kinetic stability is **1a** > **2** > **3**. The drop in $\Delta H^{\ddagger}$, from 10 to ~6 kcal/mol, is more pronounced, with a concomitant decrease of $\Delta S^{\ddagger}$ from −1.5 to −10.7 eu. While it is reasonable to suggest that less bond cleavage (decreasing $\Delta H^{\ddagger}$) and more solvation (increasingly negative $\Delta S^{\ddagger}$) in the transition state correlate with the apparent decrease in anion donor ability on going from SbF_6^- to BF_4^- to PF_6^-, the *explanation* for these changes is not obvious. As noted above the difficulty that arises is whether the ionization is dissociative or associative. If we use the picture of a continuum where no clear boundary between dissociative and associative substitution exists, explanations for the proposed relative absence of solvation in the transition state for intramolecular exchange in **1a** could involve the larger size of SbF_6^- as well as the greater degree of negative charge residing on the fluorine atoms[31] of SbF_6^-, relative to BF_4^- and PF_6^-. Each of these factors will inhibit nucleophilic solvation and lead to a later transition state, where more bond cleavage has occurred. Another plausible explanation involves the depth and width of the potential energy well that describes the W–F bond (Figure 10); the stronger W–$FSbF_5$ interaction may have a relatively narrow, deep well, and the weaker W–FPF_5 interaction may have a relatively wide, shallow well.[32] In the latter case, relatively less bond cleavage could lead to a greater "looseness" in the bond and hence allow greater access to solvent which would serve to stabilize the transition state at an earlier stage of bond cleavage.

In the SbF_6^- isokinetic group, $\Delta G^{\ddagger}$ increases from ~10.4 kcal/mol for **1a** to ~11.2–11.4 kcal/mol for **1b**. Since the W–F bond strengths must be comparable in both adducts, the increase in activation energy is presumably entropy-driven. However, solvent participation in the transition state would be expected to *decrease* with increasing steric bulk and decreasing solvent polarity, in contrast to the observed increasingly negative $\Delta S^{\ddagger}$. One possibility is that freezing out not of solvent but of phosphine ligand motion is correlated with increasing steric bulk and decreasing solvent polarity, perhaps due to agostic interactions, although why this yields increasingly "early" transition states is unclear. Since the isokinetic correlation itself is imperfect, and since there is clearly room for more experimentation with other bulky ligands as well as use of BF_4^- and PF_6^- with these ligands, further speculation is unwarranted.

Intermolecular Anion Exchange. While the activation parameters for the high-temperature intermolecular exchange process are nearly the same in each reaction, having gone through the above isokinetic analysis, it is instructive to do the same here. As shown in Figure 11, a good linear correlation of $\Delta H^{\ddagger}$ with $\Delta S^{\ddagger}$ is seen,[33] but that this is due to statistical artifact rather than an

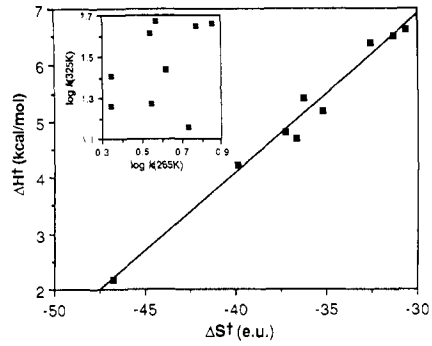

Figure 11. Isokinetic plot of intermolecular exchange activation parameters, and inset plot of log of the intermolecular exchange rate at 325 K versus that at 265 K.

Scheme V

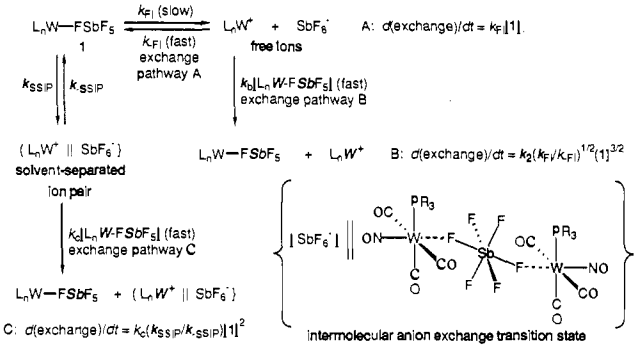

isokinetic relationship is seen by the inset plot of log k_2 versus log k_1, which reveals no correlation whatever. The major surprise, then, is that the free energy for each of these ionization reactions is essentially the same, ~14.5 kcal/mol at 260 K. This implies a similar reaction in each case (that is, one in which similar bonds are broken), which would arise in the ionic spinning mechanism where ion-pair formation has already occurred, but not in the concerted spinning mechanism where the covalent adduct would still be the predecessor for the high-temperature ionization. The enthalpic contribution is small as well as constant, implying that the forces binding the putative ion pair **4** are comparably weak in each case. The value for $\Delta S^{\ddagger}$ is not surprising for the methylene chloride reactions, where solvation of a transition state leading to the free ions would be expected to be important. The large negative numbers are well precedented by the well-known freezing effect of nonpolar solvents, where the entropy of freezing is typically twice as large as that of a well-ordered solvent such as water.[34] This might suggest that the entropy for hexane should be even *more* negative, and while this is, in fact, the case, it is nevertheless quite surprising that the values for hexane are so similar. We therefore now examine this in a quantitative manner.

A number of expressions for the free energy of dissociation of ion pairs to free ions have been derived.[1,2,12a,35] Typically, K_D, the equilibrium constant for dissociation of contact ion pairs to free ions, is calculated from consideration of the Coulombic force required to separate two charged particles in a solvent whose polarity is treated as a continuum. While differing in detail, agreement with experiment is generally good, and our purpose here is simply to compare expectations for two solvents of different dielectric constant; the relative values, which will not vary widely, are the key issue. We will use the expression due to Fuoss[2b] in eq 5,

$$K_D = [3000/4\pi N]a^{-3} \exp(-b) = 3.964 \times 10^2\, \text{Å}^{-3} \exp(-b) \quad (5)$$

(31) Teramae, H.; Tanaka, K.; Yamabe, T. *Solid State Commun.* **1982**, *44*, 431–434.

(32) Such a correlation of potential well depth and width is not theoretically required, but is commonly assumed; see, for instance: Basolo, F.; Pearson, R. G. *Mechanisms of Inorganic Reactions*, 2nd ed.; Wiley: New York, 1967; p 539.

(33) The plot of $\Delta H^{\ddagger}$ versus $\Delta S^{\ddagger}$ gives $\beta = 281 \pm 15$ K ($R = 0.990$), while the mean reaction temperature is 299.8 K.

(34) Moore, J. W.; Pearson, R. G. *Kinetics and Mechanism*, 3rd ed.; Wiley: New York, 1981; Chapter 7.

(35) Denison, J. T.; Ramsey, J. B. *J. Am. Chem. Soc.* **1955**, *77*, 2615–2621.

$$b = e^2/a\epsilon kT$$

where N = Avogadro's number = 6.02×10^{23}, k = Boltzmann's constant = 1.381×10^{-16} erg/deg K, e = electronic charge = 4.803×10^{-10} esu, ϵ is the dielectric constant of the solvent, a is the closest contact distance of the ion pair in cm, and $\mathring{a}$ is the distance in Å, as measured from the midpoint of each ion. For **1a**, we estimate the molecular radius for the tungsten cation as 5.2 Å, for **1b** as 8.5 Å, and for the SbF_6^- ion as 3.2 Å; hence $\mathring{a}$ = 8.4 Å for **1a** and 11.7 Å for **1b**. At 260 K, eq 5 gives[36] $K_D = 5.0 \times 10^{-4}$ for **1a** and 1.4×10^{-3} for **1b** in methylene chloride, giving $\Delta G°_D$ = 3.9 and 3.4 kcal/mol, respectively. Since $\Delta\Delta G^‡$ for the intermolecular–intramolecular exchange reactions is ~4 kcal/mol, a similar thermodynamic difference in the resultant intermediates is a reasonable outcome. Thus, formation of free ions in methylene chloride constitutes a reasonable mechanism to account for intermolecular exchange, and, in fact, formation of free ions in methylene chloride is well precedented.[11] The lower barrier to free ion formation for **1b** is due to the larger cation, which disperses the charge and has the effect of lowering the Coulombic forces required to separate the ions. However, the larger size is insufficient to overcome the effect of the lower dielectric solvent hexane, where eq 5 gives[36] $K_D = 1.5 \times 10^{-13}$ for **1b**, giving $\Delta G°_D$ = 15.2 kcal/mol. Thus, here the calculation suggests that free ions do *not* form in hexane after all, since the observed activation barrier for the intermolecular exchange is ~1 kcal/mol *less* than the thermodynamic difference in the proposed intermediates; that is, the contact ion pair would have to be *more* stable than the covalent adduct (which cannot be the case since only the latter is observed) in order for the transition state energy to be higher than that of the intermediate free ions! While this is in obvious accord with our original expectation that free ions should not form in hexane, it is counter to the data that suggest that the same process is occurring in both hexane and methylene chloride.

In Scheme V we illustrate potential intermolecular anion-exchange mechanisms. The first is that which we have just described above, namely, simple rate-determining formation of free ions (k_{FI}) which then randomly recombine (k_{-FI}) in the fast-exchange step; as shown the rate would be first order in **1**. While this would not account for the maximum (at 323 K) 3-fold drop in rate at one-twentieth the concentration of **1b** in hexane, it should be pointed out that this weak concentration dependence does not rule out this mechanism, since the solvent dielectric constant (actually static permittivity, ϵ_s) also changes with concentration.[11b,c,12c,37] That is, for low dielectric constant solvents like benzene and methylene chloride, ϵ_s is well known to increase with salt concentration, and so while **1b** is not a salt, it is polar and might have a substantial effect on ϵ_s. We would predict a drop in rate of free ion formation with a drop in ϵ_s, which would be consistent with the low concentration drop in rates. We note that the reason that low-temperature exchange is insensitive to concentration could be simply that the ion pair is much less polar than the free ions, and so the rates would be less sensitive to ϵ_s. Returning to pathway B in Scheme V, a species such as the tungsten cation, even though presumably solvated, would be quite reactive and so could reasonably react with the major species present in solution (the covalent adduct) in an alternative fast-exchange step (k_b[W–FSbF$_5$]), via an anion-bridged transition state of the type shown (but without the additional SbF_6^- ion). A third mechanism could involve the solvent-separated ion pair, in which the tungsten cation, now separated from the anion by a solvent molecule, could still interact with the covalent adduct in the fast-exchange step via the illustrated transition state. These latter two pathways are chain reactions; that is, the reactive species generated in the rate-determining ionization is regenerated upon exchange with covalent **1**. Using the steady-state assumption, the rate expressions shown in Scheme V are readily derived. For the free ions route, the reaction would be 3/2 order (a 20-fold drop in concentration of **1** would give a $20^{1/2} \approx 4.5$-fold drop in rate) due to the bimolecular recombination step, while the ion-pair route would be second order due to the unimolecular recombination step, both in contrast to the observed result. One way around this would be if the exchange is not a chain reaction. While there is no reasonable way that this could occur for the free-ions route, it could in the ion-pair route if the solvent-separated SbF_6^- ion were to recombine with the regenerated tungsten cation to yield *two* molecules of the covalent adduct (and/or the contact ion pair). In order not to violate the principle of microscopic reversibility, however, this would require the additional molecule of covalent adduct to be present in the *formation* of the solvent-separated ion pair as well, so the kinetics would still be bimolecular.

An alternative possibility explicitly takes into account the fact that the covalent adduct may exist in nonpolar solvents in large aggregates;[12c,38] in particular, we can easily imagine that the *n*-octyl chains of the (*n*-octyl)$_3$P ligand of **1b** give rise to the formation of *reversed micelles* in hexane, since this phenomenon is well known for both ionic and polar nonionic compounds with long alkyl chains.[39] Thus, the presence of clusters of **1b** would keep the effective concentration nearly constant; even at the lowest concentration used (~4×10^{-3} M), the sample could easily be above the critical micelle concentration.[39b] In addition, critical micelle concentrations in reversed micelles are much less sharply defined than in aqueous micelles, so this could account for the small concentration dependence of the intermolecular exchange rates for **1b** in hexane. Thus, as long as the effective concentration is comparable at 0.076 and 0.0038 M, this intermolecular anion exchange could occur *via any bimolecular reaction—without the intermediacy of free ions—and still be first order.* A transition state like that shown in Scheme V, in which trapping of the solvent-separated ion pair occurs, would be comparable to the "special salt effect" observed in some organic systems,[3,12b] but even the contact ion pair could conceivably give rise to such bimolecular exchange. It should be pointed out that the reversed micelle hypothesis does not affect the initial ionization of the covalent adduct to the ion pair, which as noted above need not be especially polar and so can still be expected to form in hexane.

Energies of the Intermediate Ion Pairs. The activation barriers that we have measured are referenced to the ground state of the covalent adduct. We will now speculate on the energies of the intermediate ion pairs, since in combination with the barriers measured these would allow construction of the complete energy diagram. Kessler has, in fact, measured the energies of intermediate ion pairs and free ions (Scheme II),[8] but has no way to measure barriers between them. A key observation of his is that the entropy of the intermediate ion pair is less than the entropy of the transition state between it and the covalent adduct; this is inherently reasonable, since the ion pair ought to be at least as strongly solvated as the transition state in which it first forms.[40] In our systems, the isokinetic analysis shows that differences in $\Delta S^‡$ among the various reactions reflect differences in position of the transition state along the reaction coordinate. Hence, the minimum observed activation entropy should yield the best approximation of the *ion-pair solvation.* Hence, for the ion pair L(CO)$_3$(NO)W$^+$X$^-$ (L = (*n*-octyl)$_3$P, Me$_3$P; X = SbF_6^-, BF_4^-, PF_6^-) in methylene chloride, we suggest that $\Delta S°_{IP} \leq -16$ eu, the value of the intramolecular exchange parameter $\Delta S^‡$ for **1b**. Since we have not detected the ion pair by NMR in the way that Kessler has, we conservatively conclude that its concentration is less than 5% of that of the covalent adduct; hence at 260 K $\Delta G°_{IP} \geq 1.5$ kcal/mol.

Just as with the ion pair, the entropy of the free ions should be less than that of the intermolecular exchange transition state

(36) At 260 K, ϵ(methylene chloride) = 10.636 and ϵ(hexane) = 1.954, from interpolation of a plot of ln ϵ versus T; see: Morgan, S. O.; Lowry, H. H. *J. Chem. Phys.* **1930**, *34*, 2385–2432.

(37) (a) Bauge, K.; Smith, J. W. *J. Chem. Soc.* **1964**, 4244–4249. (b) Cavell, E. A. S.; Knight, P. C. *Z. Phys. Chem. (Frankfurt/Main)* **1968**, *57*, 331–334. (c) Cachet, H.; Cyrot, A.; Fekir, M.; Lestrade, J.-C. *J. Phys. Chem.* **1979**, *83*, 2419–2429.

(38) Pettit, L. D.; Bruckenstein, S. *J. Am. Chem. Soc.* **1966**, *88*, 4783–4789.

(39) (a) Fendler, J. H. *Acc. Chem. Res.* **1976**, *9*, 153–161. (b) Eiche, H.-F. *Top. Curr. Chem.* **1980**, *87*, 85–145.

(40) See ref 34, pp 256–257.

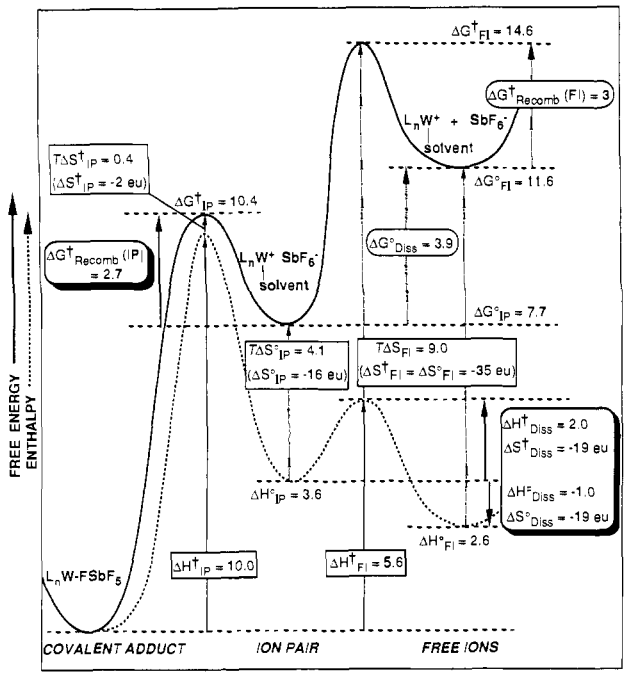

Figure 12. Reaction coordinate diagram at 260 K for free energy (solid line) and enthalpy (dotted line) of **1a**. Legend: IP, ion pair; FI, free ions; Diss, dissociation of ion pair to free ions; Recomb (FI) and Recomb (IP), recombination of free ions to ion pair, and ion pair to covalent adduct, respectively. Quantities in square boxes (ΔH, thin solid arrows; $T\Delta S$, dashed arrows) were calculated from data in Tables I–II, quantities in curved boxes (ΔG, dotted arrows) were calculated from theory (eq 5 for ΔG°_{Diss}, diffusion controlled for $\Delta G^\ddagger_{Recomb}$ (FI)[42]), and quantities in the shadowed boxes (thick solid arrows) are the principal conclusions derived from this figure.

that precedes it. Since there is no systematic variation in $\Delta S^\ddagger$ for the intermolecular exchange, we will take the best value to be the average of the nonhexane values, giving $\Delta S^\circ_{FI} \leq -35 \pm 3$ eu. We use this to obtain a value of ΔH° as follows. The rates for recombination of a number of anions and carbocations in 1,2-dichloroethane, a solvent similar to methylene chloride, were found to be diffusion controlled,[41] so for **1a** and **1b** the barrier to recombination would be ~3 kcal/mol at 260 K.[42] Since $\Delta G^\ddagger \approx 14.6$ kcal/mol, this yields $\Delta G^\circ_{FI} \approx 11.6$ kcal/mol. The above estimate of ΔS°_{FI} then yields $T\Delta S^\circ \geq 9.0$ kcal/mol, and hence $\Delta H^\circ_{FI} \leq 2.6$ kcal/mol. The complete energy diagram can be constructed now if we connect these energies to those of the ion pair, according to eq 5, where, for instance, for **1a** the free ions are 3.9 kcal/mol higher in free energy than the ion pair, giving $\Delta G^\circ_{IP} \approx 7.7$ kcal/mol, in accord with the minimum value noted above. In Figure 12 we graph the free energy and enthalpy for **1a** alone for simplicity, although we will discuss the other compounds as well.

We consider the free-energy portion of Figure 12 first. For **1a**, the barrier to ion-pair recombination is ~2.7 kcal/mol, while for **3** since $\Delta G^\ddagger_{IP} = 9.1$ kcal/mol this barrier would be ~1.4 kcal/mol, a value which suggests that the distinction here between concerted and ionic anion "spinning" is very small. We note that the PF_6^- ion is smaller than SbF_6^-, but the resultant difference in energy between ion pair and free ions is only ~0.1 kcal/mol greater, on the basis of eq 5 where $a = 8.1$ Å in **3**. For **1b** ΔG°_{IP} = ~8.2 kcal/mol since the free ions are calculated to be only 3.4 kcal/mol higher than the ion pair, so in combination with the higher barrier $\Delta G^\ddagger_{IP} = 11.2$ kcal/mol, a recombination barrier of ~3.0 kcal/mol is derived. Overall, then, the apparent barrier to recombination of the ion pair is 1.4–3.0 kcal/mol, giving rate constants for collapse of the ion pair of 10^{10}–10^{11} s^{-1}. While this is in the same range as recent estimates for "organic" ion pairs,[6b] it is of interest that in this case the anion must explicitly displace a solvent molecule for recombination to occur.

The activation barrier between ion pair and free ions is 6.9 kcal/mol for the Me_3P compounds **1a**, **2**, and **3**, and 6.4 kcal/mol for the bulkier (n-octyl)$_3$P compound **1b**. However, since this value is entropy driven, it is more interesting to compare the enthalpies and entropies. Given $\Delta G^\circ_{IP} = 7.7$ kcal/mol for **1a** and 8.2 kcal/mol for **1b**, and $\Delta S^\circ_{IP} = -15.7$ eu[43] (giving $T\Delta S = 4.1$ kcal/mol), we can calculate $\Delta H^\circ_{IP} = 3.6$ and 4.1 kcal/mol, respectively. Hence, the *difference* in ion-pair and free-ion parameters, that is, the *dissociation* parameters, are for **1a**, **2**, and **3**, $\Delta H^\circ_D = -1.0$ kcal/mol and $\Delta S^\circ_D = -18.9$ eu, and for **1b**, $\Delta H^\circ_D = -1.5$ kcal/mol and $\Delta S^\circ_D = -18.9$ eu. These numbers can be compared to theory as well. Since differentiation of the free energy with respect to temperature ultimately yields the enthalpy and entropy, eq 6 and 7 are readily derived from eq 5,[5a,12a,35,44] where

$$\Delta H^\circ_D = \frac{Re^2}{a\epsilon k}\left(1 + \frac{\partial \ln \epsilon}{\partial \ln T}\right) \quad (6)$$

$$\Delta S^\circ_D = R\left[\ln (3000/4\pi Na^3) + \frac{e^2}{a\epsilon k}\frac{\partial \ln \epsilon}{\partial T}\right] \quad (7)$$

it is assumed that the dielectric constant is the only temperature-dependent variable. Using literature data to obtain values for the derivatives[45] gives for **1a** $\Delta H^\circ_D = -1.2$ kcal/mol and $\Delta S^\circ_D = -19.6$ eu, and for **1b** $\Delta H^\circ_D = -0.8$ kcal/mol and $\Delta S^\circ_D = -16.2$ eu, values that are remarkably similar to those derived from the above analysis. Literature data[46] for the equilibrium between ion pairs and free ions of $Ph_3C^+X^-$ ($X^- = SbF_6^-$, AsF_6^-, $SbCl_6^-$, $SbCl_5OH^-$, and ClO_4^-) in methylene chloride and 1,2-dichloroethane are in excellent agreement with theory. The *experimentally* determined values for these compounds are $\Delta H^\circ_D = -0.5$ to -2.2 kcal/mol and $\Delta S^\circ_D = -17$ to -25 eu, which are similar to our values as expected since a in eq 5–7 is comparable to that for **1a**. We conclude that the use of theory to give the free energy difference between the ion pair and free ions is valid, and that the further agreement between the derived theoretical enthalpy and entropy of dissociation with our values justifies our proposal to equate ΔS° with the minimum observed $\Delta S^\ddagger$. It is also instructive to compare Figure 12 to the diagram in Scheme II due to Kessler,[8b] where the medium is the strongly ionizing solvent SO_2.[4] Differences that clearly arise due to higher solvent polarity include (1) the apparently lower activation barrier for separation of the ion pair, (2) the increased stability of both the ion pair and free ions, and (3) the somewhat higher entropy of the free ions, which is understandable on the basis of the greater freezing effect in less polar methylene chloride as noted above. The entropy of the ion pairs is not very different, nor is the energy of the initial ionization, in accord with our expectation that these two steps involve less polar species and so should be less sensitive to solvent polarity.

The theoretical equations used assume that the dielectric medium is a continuum (that is, no specific solute–solvent interactions are accounted for), so the calculated values for the entropy and enthalpy cannot reflect any differences in direct coordination of

(41) Dorfman, L. M.; DePalma, V. M. *Pure Appl. Chem.* **1979**, *51*, 123–129.

(42) This is derived from k(diffusion controlled) = 1.48 and 1.86 × 10^{10} M^{-1} s^{-1} at 260 K for **1a** and **1b** in methylene chloride; since the reactants are ions, the rate could be somewhat faster but the effect will be small. See ref 21, p 137, and Laidler, K. J. In *Chemical Kinetics*, 3rd ed.; Harper & Row: New York, 1987; pp 212–220.

(43) While the extra precision in ΔS is obviously not warranted, the extra significant figure will be used for the remainder of the discussion since it is used to give the $T\Delta S$ values.

(44) Flaherty, P. H.; Stern, K. H. *J. Am. Chem. Soc.* **1958**, *80*, 1034–1038.

(45) Data taken from ref 36 gives for methylene chloride $\partial \ln \epsilon/\partial T = -5.0474 \times 10^{-3}$ and (at 260 K) $\partial \ln \epsilon/\partial \ln T = -1.3121$, and for hexane $\partial \ln \epsilon/\partial T = -7.0180 \times 10^{-4}$ and (at 260 K) $\partial \ln \epsilon/\partial \ln T = -0.18244$.

(46) (a) Kalfoglou, N.; Szwarc, M. *J. Phys. Chem.* **1968**, *72*, 2233–2234. (b) Lee, W. Y.; Treloar, F. E. *Ibid.* **1969**, *73*, 2458–2459. (c) Bowyer, P. M.; Ledwith, A.; Sherrington, D. C. *J. Chem. Soc. B* **1971**, 1511–1514. (d) Gogolczyk, W.; Slomkowski, S.; Penczek, S. *J. Chem. Soc., Perkin Trans. 2* **1977**, 1729–1731.

solvent. The decrease in enthalpy upon ion-pair dissociation must arise because of increased favorable Coulombic interactions with the solvent, while the decrease in entropy clearly arises because of the increase in order of the solvent. The intervening transition state must reflect these factors, since we have, in fact, equated the entropy of the transition state and product free ions, giving $\Delta S^{\ddagger}_{D} \approx -19$ eu. The enthalpic barrier for conversion of the ion pair to the free ions, $\Delta H^{\ddagger}_{D}$, of only 1.5–2 kcal/mol (using $\Delta H^{\ddagger}_{FI} \approx 5.6$ kcal/mol, the average of the nonhexane values) must represent the sum of the ionic bond energies between the "noncoordinating" anions and the tungsten cations, minus a contribution for the increased enthalpy of solvation that could be ~1.5 kcal/mol on the basis of equating this contribution with ΔH°_{D}. While we are not aware of any comparable observations of the ion-pair–free ion enthalpy barrier, direct measurements of ion-pair dissociation at a single temperature by laser-flash photolysis have been reported independently by Peters and Kochi.[10c,d] Data obtained by Kochi in methylene chloride for anthracene radical cation and trinitromethide anion yield a similar free-energy barrier ($\Delta G^{\ddagger}$(20 °C) ≈ 8 kcal/mol from the solvent-separated ion pair compared to ~7 kcal/mol for **1a** from the contact ion pair) although two factors—the substantially higher barrier to ion-pair recombination from the contact ion pair (~5 kcal/mol) and the observation of a solvent-separated ion pair that is another 2 kcal/mol more stable than the contact ion pair—make further comparisons difficult.

Two further conclusions regarding solute–solvent interactions can be drawn. First, the agreement between our data and theory, even given the assumptions inherent in the derivation of Figure 12, *shows that no further coordination of solvent takes place upon formation of free ions in methylene chloride.* The alternative situation, where *additional* solvent coordination occurs upon ion-pair dissociation to free ions, has been observed, and rather than the typical values[5,35,44,46] such as those mentioned above, entropies of −50 to −60 eu are observed.[5c,d] Thus, since we expect methylene chloride will coordinate to tungsten at the free ion stage,[15] it must be coordinated already at the ion-pair stage, as depicted by **4**. The second conclusion to be drawn concerns the hexane data. We noted that a possible complication in our experiment was the possible presence of ~1 equiv of methylene chloride. While this could reasonably coordinate to the tungsten cation, it can have only a minor effect at best on the overall dielectric properties of the medium which give rise to the calculated dissociation parameters. Application of eq 6 and 7 to **1b** in hexane[45] gives ΔH°_{D} = 11.9 kcal/mol and ΔS°_{D} = −13 eu. Direct coordination of one molecule of solvent could not possibly change these numbers into values comparable to those derived above. Furthermore, if any methylene chloride were coordinated to *both* the ion pair and free ions, as might be expected if it were present, it would then contribute nothing to the observed $\Delta H^{\ddagger}$ and $\Delta S^{\ddagger}$. Thus, the conclusion that free ions do not account for intermolecular anion exchange in the hexane experiments is required.

Conclusion

We have shown that the intramolecular anion "spinning" observed in a set of tungsten adducts of "noncoordinating" anions can be best accounted for by ionization of the covalent adducts to ion pairs followed by ion pair recombination, rather than by a chelated transition state in which complete W–F bond cleavage does not occur. The activation barriers to ionization reflect differences in transition-state rather than ground-state energies, and follow the same order of adduct stability, $SbF_6^- > BF_4^- > PF_6^-$, that we have empirically observed and also confirmed on the basis of solid-state structures.[13b] This leads to the curious conclusion that the apparent coordinating ability of these anions here is a kinetic, rather than thermodynamic, property. Recombination barriers for the ion pair, which like the free ions is proposed to directly ligate a molecule of solvent, range from 1.4 to 3.0 kcal/mol, so while it is an intermediate, it is not long lived.

Intermolecular anion exchange, which might most readily be accounted for by complete ionization to free ions, occurs with similar activation parameters regardless of anion, steric bulk, and solvent, suggesting a common mechanism of diffusion of a weakly bound ion pair out of a solvent cage. However, comparison of experimental results to theoretical analyses of ion-pair dissociation as a function of solvent dielectric constant suggests that while this mechanism readily accounts for the exchange in methylene chloride, it cannot account for the exchange in hexane. We propose that reversed micelles of the trioctylphosphine-substituted complex form in hexane and that all reactions are carried out above the critical micelle concentration, thereby accounting for the nearly first-order intermolecular anion exchange which can nevertheless arise due to a bimolecular exchange reaction, possibly via contact or solvent-separated ion pairs. There is no reason to propose the existence of reversed micelles in methylene chloride, especially for the trimethylphosphine-substituted compounds, so we are forced to conclude that the similarity in activation parameters is serendipitous. Nevertheless, the apparent first-order exchange in hexane deserves further scrutiny, since the existence of this second intermolecular exchange reaction channel is apparently unprecedented.

We conclude by examining that which is unique in these systems. We have described a novel NMR method by which to measure ionization and ion-pair separation barriers, albeit with the cautionary note that too drastic a change in solvent can yield a mechanism change as suggested by reversed micelle formation in hexane. The technique provides a relatively simple alternative to measurement of barriers to separation as well as recombination of (radical) cation/anion pairs generated by laser-flash photolysis,[10] but perhaps more importantly the use of NMR allows a completely different and therefore independent means by which to measure such rate constants, albeit in systems of ion pairs generated by completely different means as well. From the transition metal viewpoint, the key feature for the use of the NMR method appears to be the presence of the phosphine reporter nucleus, which yields a phosphorus–fluorine coupling constant suitable for analysis. Fischer[47] and Beck[15b] have reported similar spectra for BF_4^- adducts. Only Beck reported variable-temperature spectra, but a line-shape analysis was not carried out, possibly owing to complications arising from an accompanying temperature-dependent cis–trans isomerization. Nevertheless, study of a relatively wide range of compounds and solvents may be possible. From the "organic" viewpoint, the key feature is our observation of the ground-state adduct alone, which undergoes observable exchange reactions and hence yields *activation barriers* for the ionization to ion pair and separation to free ions. This is in contrast to well-studied systems in which *thermodynamic equilibria* between covalent adduct and ions,[8] or between contact and solvent-separated ion pairs,[5] or between ion pairs and free ions,[8,11,35,44,46] are observed. Combination of these kinetic and thermodynamic features may be possible in the organometallic systems through the use of UV, FTIR, and conductance measurements with NMR experiments of the type that we have presented here.

Experimental Section

All manipulations of air-sensitive compounds were carried out either in a Vacuum Atmospheres inert atmosphere glovebox under recirculating nitrogen, or using standard Schlenk techniques. The low-temperature NMR spectra of **3** were recorded on a Bruker AM-360 spectrometer; all other NMR spectra were recorded on a Bruker WP-200 spectrometer. Chemical shifts are reported relative to residual $CHDCl_2$ (^{1}H, δ 5.32) in CD_2Cl_2, 8.5% H_3PO_4 in a 1-mm coaxial tube (^{31}P, 0.00 ppm) or internal $Me_3PW(CO)_5$ (^{31}P, −38.03 ppm in CD_2Cl_2). Probe temperatures were determined using a methanol standard sample according to the method of van Geet.[48] Infrared spectra were obtained in 0.1-mm NaCl solution cells on a Perkin-Elmer 237 spectrophotometer. Elemental analyses were performed by Galbraith Laboratories, Inc., Knoxville, TN. Mass spectra (EI) wre obtained on an AEI MS902.

All solvents were treated under nitrogen. Methylene chloride was distilled from phosphorus pentoxide, CS_2 and CD_2Cl_2 were vacuum-transferred from phosphorus pentoxide, and hexane was washed successively with 5% nitric acid in sulfuric acid, water, and saturated

(47) Richter, K.; Fischer, E. O.; Kreiter, C. G. *J. Organomet. Chem.* **1976**, *122*, 187–196.
(48) van Geet, A. L. *Anal. Chem.* **1970**, *42*, 679–680.

Table III. Elements of the Exchange Matrix for the R_3P NMR Multiplet for Ionic Intramolecular Exchange in **1a**, **1b**, and **3**

site	ν^a	spin state[b]	pop.[c]	transition probabilities[d]
1	$-J/2$	$\alpha(\alpha^5)$	1	1 (1)
2	$-J/2$	$\alpha(\alpha^4\beta)$	5	2 (5/6), 3 (1/6)
3	$J/2$	$\beta(\alpha^5)$	1	2 (5/6), 3 (1/6)
4	$-J/2$	$\alpha(\alpha^3\beta^2)$	10	4 (10/15), 5 (5/15)
5	$J/2$	$\beta(\alpha^4\beta)$	5	4 (10/15), 5 (5/15)
6	$-J/2$	$\alpha(\alpha^2\beta^3)$	10	6 (10/20), 7 (10/20)
7	$J/2$	$\beta(\alpha^3\beta^2)$	10	6 (10/20), 7 (10/20)
8	$-J/2$	$\alpha(\alpha\beta^4)$	5	8 (5/15), 9 (10/15)
9	$J/2$	$\beta(\alpha^2\beta^3)$	10	8 (5/15), 9 (10/15)
10	$-J/2$	$\alpha(\beta^5)$	1	10 (1/6), 11 (5/6)
11	$J/2$	$\beta(\alpha\beta^4)$	5	10 (1/6), 11 (5/6)
12	$J/2$	$\beta(\beta^5)$	1	12 (1)

[a] J (in Hz) is $^2J_{P(\mu\text{-}F)}$ for PR_3. [b] Listed in order of $(\mu\text{-F})(F_{terminal})_5$. [c] Actual population ×64. [d] For each line probability in parentheses of transition to the listed site. All other transition probabilities are zero.

aqueous sodium carbonate, and then distilled from *n*-butyllithium. Absolute ethanol was dried over 3 Å molecular sieves and purged with nitrogen immediately prior to use. Details concerning nitrosonium salts and trimethylphosphine tungsten compounds may be found in ref 13b. Tri-*n*-octylphosphine (Alfa) was used as received. Glassware used with the title compounds was oven-dried overnight at 140 °C and transferred into the glovebox while still hot.

(*n*-octyl)$_3$PW(CO)$_5$. A suspension of 0.31 g (0.9 equiv) of (*n*-octyl)$_3$P in 5 mL of ethanol was added to a suspension of 0.50 g of $BrW(CO)_5^-NEt_4^+$ in 20 mL of ethanol.[49] After stirring at room temperature for 50 min, the resultant clear yellow solution was stripped on a vacuum line, giving a yellow solid and oil. This material was extracted with 5 × 8 mL of hexane and the solution was stripped to give 0.51 g (87% yield) of product as a yellow oil: IR (hexane) 2060 (m), 1940 (vs), 1900 (mw), 1875 (mw) cm^{-1}; ^{1}H NMR (CD_2Cl_2) δ 1.79 (m, 6 H, CH_2P), 1.42 (m, 6 H), 1.29 (s, 30 H), 0.89 (m, 9 H, CH_3); ^{31}P NMR (CD_2Cl_2, 306 K) −5.95 ($^1J_{PW}$ = 229 Hz) ppm; MS (16 eV) *m/e* (for ^{184}W) 694 (M^+, 100%), 666 (M^+ − CO, 9%), 638 (M^+ − 2 CO, 9%). Anal. Calcd for $C_{29}H_{51}O_5PW$: C, 50.15; H, 7.40. Found: C, 51.28; H, 7.25.

Sample Preparation. Compound **1a** was made according to ref 13b. Compounds **1b**, **2**, and **3** were made in situ as follows. Solid NO^+X^- (X^- = SbF_6^-, BF_4^-, PF_6^-, 1–1.7 equiv) was added to a solution of $R_3PW(CO)_5$ (R = Me, *n*-octyl) in CD_2Cl_2 and the suspension stirred until cessation of bubbling, usually 15–45 min. The yellow solutions were then filtered through oven-dried Celite in a pipet column directly into the NMR tube. Spectral data for **1a**, **2**, and **3** may be found in ref 13b; for **1b** (which was an oil) data are as follows: IR (CH_2Cl_2) 2105 (mw), 2015 (m), 1695 (m) cm^{-1}; ^{31}P NMR (CD_2Cl_2, 305.1 K) 8.70 (br septet, $^2J_{PF}$ = 34.2 Hz, $^1J_{PW}$ = 281 Hz) ppm; (CD_2Cl_2, 193.7 K) 7.25 (d, $^2J_{PF}$ = 31.6 Hz, $^1J_{PW}$ = 277 Hz) ppm; (hexane, 284.5 K) 7.79 (br septet, $^2J_{PF}$ = 35.7 Hz, $^1J_{PW}$ = 281 Hz) ppm; (hexane, 193.7 K) 8.45 (d, $^2J_{PF}$ = 33.2 Hz, $^1J_{PW}$ = 279 Hz) ppm.

The low-temperature spectra on **3** were run in a 5-mm NMR tube; all others were run in 10-mm tubes or (for all the intermolecular exchange data) in sealed 8-mm tubes. For the samples of **1b** in protiohexane, the sealed 8-mm tube was centered in a 10-mm tube using Teflon tape, and a deuterated solvent (acetone-d_6 or toluene-d_8) added to the outer tube to provide the deuterium-lock signal. Sample shimming was accomplished by maximizing the proton FID of the hexane solvent. The high-concentration sample of **1b** was prepared by carrying out the reaction in CH_2Cl_2, stripping the sample on a vacuum line for 1 h, and redissolving in hexane and filtering the sample into the NMR tube. In order to minimize sample decomposition upon concentration,[13b] the low-concentration sample of **1b** was prepared by adding hexane to the original sample of **1b** in 2 mL of CH_2Cl_2 to a total volume of 10 mL, concentrating to 4 mL, and then repeating the filling to 10 mL with hexane and concentrating to 4 mL three more times.

Line-Shape Analyses. Calculations were carried out on a VAX 780 computer using a program for multisite exchange without coupling.[50] Calculated spectra were visually compared to experimental spectra in order to determine the best fit rate constants. For the low-temperature exchange, rate constants in Table I were determined with a precision of ~2–5% over the range $k \approx 60$–5000 s^{-1} and to within ~10% for lower rates, while for the high-temperature exchange, rate constants in Table II were determined to within ~10–20%; within these percentage ranges

(49) Schenk, W. A. *J. Organomet. Chem.* **1979**, *179*, 253–261.

(50) NMR line-shape program written by F. A. L. Anet, 1975, and modified by S. S. Muira for output to an HP plotter, 1984.

Table IV. Elements of the Exchange Matrix for the R_3P NMR Multiplet for Intramolecular Exchange in **2**

site	ν^a	spin state[b]	pop.[c]	ionic trans. probabilities[d]	concerted trans. probabilities[d]
1	$-J/2$	$\alpha(\alpha^3)$	1	1 (1)	1 (1)
2	$-J/2$	$\alpha(\alpha^2\beta)$	3	2 (3/4), 3 (1/4)	2 (2/3), 3 (1/3)
3	$J/2$	$\beta(\alpha^3)$	1	2 (3/4), 3 (1/4)	2 (1)
4	$-J/2$	$\alpha(\alpha\beta^2)$	3	4 (2/4), 5 (2/4)	4 (1/3), 5 (2/3)
5	$J/2$	$\beta(\alpha^2\beta)$	3	4 (2/4), 5 (2/4)	4 (2/3), 5 (1/3)
6	$-J/2$	$\alpha(\beta^3)$	1	6 (1/4), 7 (3/4)	7 (1)
7	$J/2$	$\beta(\alpha\beta^2)$	3	6 (1/4), 7 (3/4)	6 (1/3), 7 (2/3)
8	$J/2$	$\beta(\beta^3)$	1	8 (1)	8 (1)

[a] J (in Hz) is $^2J_{P(\mu\text{-}F)}$ for PR_3. [b] Listed in order of $(\mu\text{-F})(F_{terminal})_3$. [c] Actual population ×16. [d] For each line probability in parentheses of transition to the listed site. All other transition probabilities are zero.

Table V. Elements of the Exchange Matrix for the R_3P NMR Multiplet for Concerted Intramolecular Exchange in **1a**, **1b**, and **3**

site	ν^a	spin state[b]	pop.[c]	transition probabilities[d]
1	$-J/2$	$\alpha(\alpha^4)\alpha$	1	1 (1)
2	$-J/2$	$\alpha(\alpha^4)\beta$	1	3 (1)
3	$-J/2$	$\alpha(\alpha^3\beta)\alpha$	4	2 (1/4), 3 (2/4), 4 (1/4)
4	$J/2$	$\beta(\alpha^4)\alpha$	1	3 (1)
5	$-J/2$	$\alpha(\alpha^3\beta)\beta$	4	5 (1/4), 6 (2/4), 7 (1/4)
6	$-J/2$	$\alpha(\alpha^2 cis\text{-}\beta^2)\alpha$	4	5 (2/4), 7 (2/4)
7	$J/2$	$\beta(\alpha^3\beta)\alpha$	4	5 (1/4), 6 (2/4), 7 (1/4)
8	$-J/2$	$\alpha(\alpha^2 trans\text{-}\beta^2)\alpha$	2	8 (2/4), 9 (2/4)
9	$J/2$	$\beta(\alpha^4)\beta$	1	8 (1)
10	$-J/2$	$\alpha(\alpha^2 cis\text{-}\beta^2)\beta$	4	10 (2/4), 11 (2/4)
11	$J/2$	$\beta(\alpha^2 cis\text{-}\beta^2)\alpha$	4	10 (2/4), 11 (2/4)
12	$-J/2$	$\alpha(\alpha^2 trans\text{-}\beta^2)\beta$	2	13 (2/4), 15 (2/4)
13	$-J/2$	$\alpha(\alpha\beta^3)\alpha$	4	12 (1/4), 14 (1/4), 15 (2/4)
14	$J/2$	$\beta(\alpha^2 trans\text{-}\beta^2)\alpha$	2	13 (2/4), 15 (2/4)
15	$J/2$	$\beta(\alpha^3\beta)\beta$	4	12 (1/4), 13 (2/4), 14 (1/4)
16	$J/2$	$\beta(\alpha\beta^3)\alpha$	4	16 (1/4), 17 (2/4), 18 (1/4)
17	$J/2$	$\beta(\alpha^2 cis\text{-}\beta^2)\beta$	4	16 (2/4), 18 (2/4)
18	$-J/2$	$\alpha(\alpha\beta^3)\beta$	4	16 (1/4), 17 (2/4), 18 (1/4)
19	$J/2$	$\beta(\alpha^2 trans\text{-}\beta^2)\beta$	2	19 (2/4), 20 (2/4)
20	$-J/2$	$\alpha(\beta^4)\alpha$	1	19 (1)
21	$J/2$	$\beta(\beta^4)\alpha$	1	22 (1)
22	$J/2$	$\beta(\alpha\beta^3)\beta$	4	21 (1/4), 22 (2/4), 23 (1/4)
23	$-J/2$	$\alpha(\beta^4)\beta$	1	22 (1)
24	$J/2$	$\beta(\beta^4)\beta$	1	24 (1)

[a] J (in Hz) is $^2J_{P(\mu\text{-}F)}$ for PR_3. [b] Listed in order of $(\mu\text{-F})(F_{equatorial})_4$-$(F_{axial})$. [c] Actual population ×64. [d] For each line probability in parentheses of transition to the listed site. All other transition probabilities are zero.

Table VI. Elements of the Exchange Matrix for the R_3P NMR Multiplet for Intermolecular Exchange[a]

1a, **1b**, and **3**				**2**			
site	ν^b	spin state[c]	pop.[d]	site	ν^b	spin state[e]	pop.[f]
1	$-J/2$	α^6	1	1	$-J/2$	α^4	1
2	$-J/3$	$\alpha^5\beta$	6	2	$-J/4$	$\alpha^3\beta$	4
3	$-J/6$	$\alpha^4\beta^2$	15	3	0	$\alpha^2\beta^2$	6
4	0	$\alpha^3\beta^3$	20	4	$J/4$	$\alpha\beta^3$	4
5	$J/6$	$\alpha^2\beta^4$	15	5	$J/2$	β^4	1
6	$J/3$	$\alpha\beta^5$	6				
7	$J/2$	β^6	1				

[a] For each site the transition probability for exchange to any site *n* is equal to the population of site *n*. [b] J (in Hz) is $^2J_{P(\mu\text{-}F)}$ for PR_3. [c] For SbF_6^- and PF_6^-. [d] Actual population ×64. [e] For BF_4^-. [f] Actual population ×16.

little or no visual difference between calculated spectra could be detected. In all cases the line width of the $Me_3PW(CO)_5$ signal was used to determine T_2; this leads in principle to the greatest uncertainties occurring in rate constants at the slow- and fast-exchange limits.[19] In practice, the least certain rates were those at the fast-exchange limit of the intramolecular exchange, on the basis of large deviations of this last point from the Eyring plots. The highest temperature used overall for these plots, therefore, was ~250 K with the exception of **2** where the deviation was already high at that temperature, and **3** where the fast-exchange limit was reached at 220 K. This is different from results originally published for **1a** ($\Delta H^\ddagger$ = 8.9 ± 0.2 kcal/mol and $\Delta S^\ddagger$ = −6.4 ± 0.8 eu)[13a] where

Table VII. Elements of the Exchange Matrix for the W-FPF_5 NMR Multiplet for Ionic Intramolecular Exchange in **3**

site	ν^a	spin state[b]	pop.[c]	transition probabilities[d]
1	-2190.37	$\alpha(\alpha^4)\alpha$	1	1 (1)
2	-1693.51	$\beta(\alpha^4)\alpha$	1	2 (1/6), 3 (1/6), 4 (4/6)
3	-1426.41	$\alpha(\alpha^4)\beta$	1	2 (1/6), 3 (1/6), 4 (4/6)
4	-1410.39	$\alpha(\alpha^3\beta)\alpha$	4	2 (1/6), 3 (1/6), 4 (4/6)
5	-929.55	$\beta(\alpha^4)\beta$	1	5 (1/15), 6 (4/15), 7 (4/15), 8 (6/15)
6	-913.53	$\beta(\alpha^3\beta)\alpha$	4	5 (1/15), 6 (4/15), 7 (4/15), 8 (6/15)
7	-646.43	$\alpha(\alpha^3\beta)\beta$	4	5 (1/15), 6 (4/15), 7 (4/15), 8 (6/15)
8	-630.41	$\alpha(\alpha^2\beta^2)\alpha$	6	5 (1/15), 6 (4/15), 7 (4/15), 8 (6/15)
9	-149.57	$\beta(\alpha^3\beta)\beta$	4	9 (4/20), 10 (6/20), 11 (6/20), 12 (4/20)
10	-133.55	$\beta(\alpha^2\beta^2)\alpha$	6	9 (4/20), 10 (6/20), 11 (6/20), 12 (4/20)
11	133.55	$\alpha(\alpha^2\beta^2)\beta$	6	9 (4/20), 10 (6/20), 11 (6/20), 12 (4/20)
12	149.57	$\alpha(\alpha\beta^3)\alpha$	4	9 (4/20), 10 (6/20), 11 (6/20), 12 (4/20)
13	630.41	$\beta(\alpha^2\beta^2)\beta$	6	13 (6/15), 14 (4/15), 15 (4/15), 16 (1/15)
14	646.43	$\beta(\alpha\beta^3)\alpha$	4	13 (6/15), 14 (4/15), 15 (4/15), 16 (1/15)
15	913.53	$\alpha(\alpha\beta^3)\beta$	4	13 (6/15), 14 (4/15), 15 (4/15), 16 (1/15)
16	929.55	$\alpha(\beta^4)\alpha$	1	13 (6/15), 14 (4/15), 15 (4/15), 16 (1/15)
17	1410.39	$\beta(\alpha\beta^3)\beta$	4	17 (4/6), 18 (1/6), 19 (1/6)
18	1426.41	$\beta(\beta^4)\alpha$	1	17 (4/6), 18 (1/6), 19 (1/6)
19	1693.51	$\alpha(\beta^4)\beta$	1	17 (4/6), 18 (1/6), 19 (1/6)
20	2190.37	$\beta(\beta^4)\beta$	1	20 (1)

[a] In Hz, relative to chemical shift of 0 Hz. [b] Listed in order of (μ-F)($F_{equatorial}$)$_4$(F_{axial}). [c] Actual population ×64. [d] For each line probability in parentheses of transition to the listed site. All other transition probabilities are zero.

the rate constant at 264.9 K on the basis of exclusive intramolecular exchange was determined to be 9000 s^{-1} and was used in the Eyring plot, but broadening from intermolecular exchange must be present so we have deleted this point here. In all cases, the error limits on the activation parameters were derived from the standard deviations of the slope and intercept of the least-squares fit straight line to the data.

The ionic exchange mechanism was treated as a 12-site exchange problem for the SbF_6^- and PF_6^- adducts and as an 8-site problem for BF_4^- adduct **2**. Elements of the exchange matrices are listed in Tables III and IV including the NMR exchange site number, frequency, fluorine spin state, population, and nonzero transition probabilities. The concerted mechanism for **2** is also an 8-site problem and as described in the text differs little from the ionic mechanism; elements of this exchange matrix are in Table IV. The concerted mechanism for the octahedral anions must be treated as a 24-site exchange problem since the axial, and cis- and trans-equatorial spin sites are in principle different; elements of this exchange matrix are in Table V. The intermolecular exchange mechanism, treated as described in the text, reduces to a 7-site problem for **1a**, **1b**, and **3**, and a 5-site problem for **2**, as shown in Table VI. Lastly, the calculation of the PF_6^- spectra in Figure 6 was treated as a 20-site exchange problem. Coupling constants from the ^{19}F NMR spectra of **3**[13b] ($J_{(\mu\text{-}F)P}$ = 496.86 Hz, $J_{F(equatorial)P}$ = 779.98 Hz, and $J_{F(axial)P}$ = 763.96 Hz) were combined to give precise expected positions of a doublet of doublet of quintets, and elements of the exchange matrix are listed in Table VII.

Acknowledgment. We thank Professor F. A. L. Anet for helpful discussions and assistance in setting up the line-shape analysis, Professor J. A. Gladysz for a preprint of ref 15f, and one of the referees for insightful comments. Financial support was provided by the donors of the Petroleum Research Fund, administered by the American Chemical Society, Chevron Research Co., the UCLA Committee on Research, and a Biomedical Research Support Grant.

Catalysis of Diels-Alder Reactions by Low Oxidation State Transition-Metal Lewis Acids: Fact and Fiction

Peter V. Bonnesen, Craig L. Puckett, Robert V. Honeychuck, and William H. Hersh*

Contribution from the Department of Chemistry and Biochemistry, University of California, Los Angeles, California 90024-1569. *Received September 12, 1988*

Abstract: Catalysis of Diels-Alder reactions between the dienes cyclopentadiene, butadiene, isoprene, and piperylene and the enones acrolein, methyl vinyl ketone, and methyl acrylate is induced by 0.1-2.5 mol % of *mer*-(*cis*-Me_3P)(*trans*-NO)-$(CO)_3W(\mu\text{-}F)SbF_5$ (**1**), $(Cy_2PCH_2CH_2PPh_2)(CO)_2(NO)W(\mu\text{-}F)SbF_5$ (**2**), $Cp(CO)_2FeL^+X^-$ (L = THF, X^- = BF_4^-, **3a**; X^- = SbF_6^-, **3b**; L = η^1-acrolein, X^- = PF_6^-, **3d**), or $Cp(CO)_2L'ML^+PF_6^-$ (L' = CO, L = acrolein, M = Mo, **4a**; L' = PPh_3, L = THF, M = Mo, **4b**; L' = CO, L = THF, M = W, **4c**). Enhancement of rates and regio- and stereoselectivity is observed compared to the thermal reactions; the order of apparent catalytic activity is **1** > **2** ≈ **3a** > **4a**, **4c**. The order of Lewis acidity is **1** > **2** > **4a** > **3a**, casting doubt on the role of $Cp(CO)_2Fe^+$ in catalysis. The potential impurity $Ag^+BF_4^-$ is similarly reactive, although not in lower concentrations. Use of 2,6-di-*tert*-butylpyridine (**5**) and 1-(*n*-butyl)-2,2,6,6-tetramethylpiperidine (**6**) as hindered bases to trap Ag^+ and H^+ in the presence of transition-metal Lewis acids is described. Substoichiometric use of **5** demonstrates that $Ag^+BF_4^-$ is not the real catalyst and that the true activity of **3a** is low. Use of **5** with stronger acids, namely the acrolein adduct of **1** (**1a**) and **4a**, or of the stronger base **6** with **3a** leads to catalyst destruction, via a pathway proposed to involve deprotonation of coordinated methylene chloride. The reactivity of other potential impurities (HBF_4·Et_2O, BF_3·Et_2O, $Ph_3C^+PF_6^-$, and $NO^+SbF_6^-$) is briefly examined, as is that of analogues of **3a** that have different counterions. Kinetic analysis of stoichiometric reactions of metal-acrolein adducts with isoprene shows that the relative rates of cycloaddition for **1a**, the acrolein adduct of **2**, **4a**, and **3d** are 68:20:8:1 and that the rate-determining step in the catalytic reactions is the rate of aldehyde turnover. The calculated rate constants are used to predict catalytic yields and demonstrate that **1** and **2** can be the real catalysts. For **3a** and possibly **4a** as well, the observed catalytic activity is significantly greater than expected on the basis of the stoichiometrically determined rate constants, so the real catalysis in these cases apparently is due to the presence of much more reactive materials present as impurities.

We recently reported[1] that Diels-Alder reactions between butadiene or cyclopentadiene and α,β-unsaturated enones may be catalyzed by as little as 0.1 mol % of the tungsten nitrosyl Lewis acid $Me_3P(CO)_3(NO)W(\mu\text{-}F)SbF_5$ (**1**)[2] and that the mode of catalysis is likely due to activation of the α,β-unsaturated enone by simple η^1-carbonyl coordination, on the basis of an X-ray structure of the tungsten-acrolein adduct **1a**. Since we were aware of related η^1-adducts of the metal fragments $Cp(CO)_2Fe^+$

(1) Honeychuck, R. V.; Bonnesen, P. V.; Farahi, J.; Hersh, W. H. *J. Org. Chem.* **1987**, *52*, 5293-5296.

(2) (a) Hersh, W. H. *J. Am. Chem. Soc.* **1985**, *107*, 4599-4601. (b) Honeychuck, R. V.; Hersh, W. H. *Inorg. Chem.*, in press.

0002-7863/89/1511-6070$01.50/0